Alma Mater Studiorum – Università di Bologna

DOTTORATO DI RICERCA IN

Scienze Biomediche e Neuromotorie

Ciclo XXXV

Settore Concorsuale: 05/D1

Settore Scientifico Disciplinare: BIO/09

RELATIVE INFLUENCE OF GAZE AND STATIC ARM POSITION IN THE SUPERIOR PARIETAL LOBULE OF THE MACAQUE MONKEY DURING REACHING

Presentata da: Marta Tabanelli

Coordinatore Dottorato

Prof.ssa Matilde Yung Follo

Supervisore

Prof.ssa Patrizia Fattori

Co-supervisore

Prof.ssa Rossella Breveglieri

Esame finale anno 2023

INDEX

1. ABSTRACT

The superior parietal lobule (SPL) of macaques is classically described as an associative cortex implicated in visuospatial perception, planning and control of reaching and grasping movements (De Vitis et al., 2019; Galletti et al., 2003, 2018, 2022; Fattori et al., 2017; Hadjidimitrakis et al., 2015). These processes are the result of the integration of signals related to different sensory modalities.

During a goal-directed action, eye and limb information are combined to ensure that the hand is transported at the gazed target location and the arm is maintained steady in the final position. The SPL areas V6A, PEc and PE contain cells sensitive to the direction of gaze and limb position but less is known about the degree of independent encoding of these signals. In this thesis, we evaluated the influence of eye and arm position information upon single neuron activity of areas V6A, PEc and PE during the holding period after the execution of arm reaching movement, when the gaze and hand are both still at the reach target. Two male macaques (*Macaca fascicularis*) performed a reaching task while single unit activity was recorded from areas V6A, PEc and PE. We found that neurons in all these areas were modulated by eye and static arm positions with a joint encoding of gaze and somatosensory signals in V6A and PEc and a mostly separate processing of the two signals in PE.

The elaboration of this information reflects the functional gradient found in the SPL with the caudal sector characterized by visuo-somatic properties in comparison to the rostral sector dominated by somatosensory signals. This evidence well agree also with the recent reallocation of areas V6A and PEc in Brodmann's area 7 depending on their similar structural and functional features with respect to PE belonging to Brodmann's area 5 (Gamberini et al., 2020).

2. HIGHLIGHTS

- ❖ In the Superior Parietal Lobule (SPL), eye and arm position signals are processed more jointly in caudal areas V6A and PEc than in rostral area PE.
- ❖ The integration of eye and arm position signals used to control limb posture, at the end of a reaching movement, follows a functional trend that mimics the visuo-somatic gradient already found in the SPL.
- ❖ The similarity of the functional properties of V6A and PEc, supports their recent allocation in the same area (Brodmann area 7).
- ❖ The different functional properties of PE is consistent with its location within a different cytoarchitectural region (Brodmann area 5).

3. INTRODUCTION

3.1 Posterior Parietal Cortex and eye-hand coordination

A peculiar characteristic of primates is their ability to coordinate eye and hand positions to perform accurate movements using their hands to interact with the environment. Typically, during reaching, the eyes are directed to the desired target before the arm movement takes place (Land and Hayhoe 2001) and their position is kept stable on it. Noteworthy, movements become less accurate in situations in which the eyes are not allowed to move to the object of interest (Prablanc et al., 1979; Abrams et al., 1990). Therefore, the brain profits from the foveal fixation of the target which is likely to guide the arm to the correct final position, at the object location. At the end of the movement, when the hand is on the target, a match between visual and proprioceptive maps takes place, as a result of the concurrent elaboration in the brain of eye and hand position signals (Soechting & Flanders ,1989).

The posterior parietal cortex (PPC), a key node for the integration of multi-sensory signals, was particularly investigated in the past for its suggested higher role in elaborating these stimuli during voluntary arm movements (Kalaska et al., 1997; Caminiti et al., 1998; Colby and Goldberg, 1999; Andersen and Buneo, 2002; Galletti et al., 2003).

The PPC occupies the caudal part of the parietal lobe in both humans and non-human primates, it is located just posteriorly to the anterior parietal cortex (APC) which also hosts the primary somatosensory cortex (S1) (Figure 1). The PPC projects primarily to the premotor areas of the frontal lobe, providing pathways for initiating and controlling motor behaviour. These frontal–parietal networks play a crucial role in voluntary movements, particularly the skilled movements of the hand and arm such as reaching, grasping, and tool use (Matelli and Luppino, 2001; Battaglia-Mayer et al., 2003).

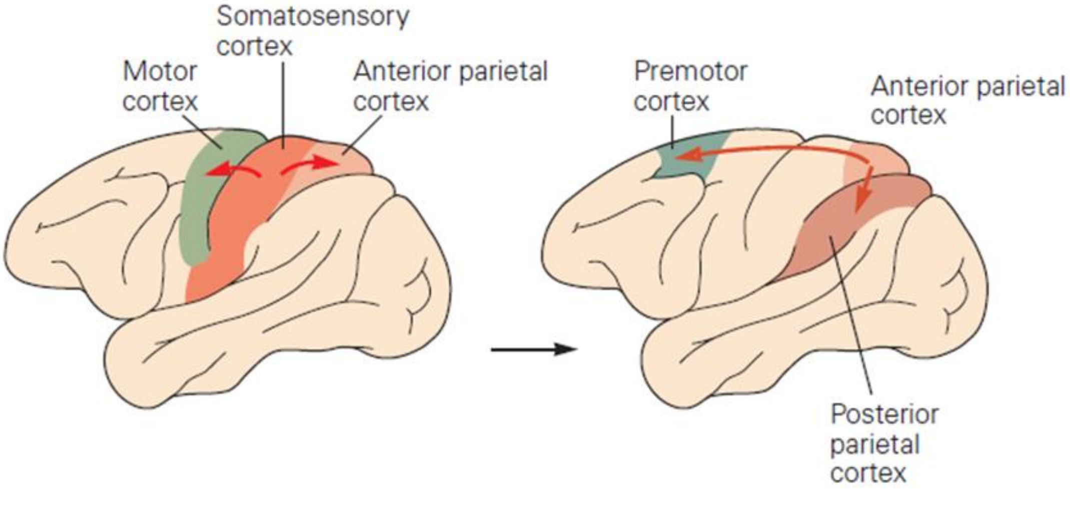

Figure 1. Schematic processing of sensory information in the macaque cerebral cortex. *The primary somatosensory cortex projects to the motor area in the frontal lobe and to the somatosensory association area in the parietal cortex. The somatosensory association area, in turn, projects to higher-order somatosensory association areas in the posterior parietal cortex and to the premotor cortex (modified from Kandel et al. 2014).*

The PPC has been subdivided into a Superior Parietal Lobule (SPL), which extends medially and on the mesial surface of the cerebral hemisphere and an Inferior Parietal Lobule (IPL) separated from the SPL by the intraparietal sulcus.

According to the “Two Visual Systems Hypothesis”, visual stimuli leave the primary visual cortex following two main pathways: a dorsal one directed to the PPC, and a ventral one that reaches the inferior temporal lobe (Ungerleider and Mishkin, 1982). Originally, the functional role of the PPC, in the so called “dorsal visual stream” was thought to convey spatial information for stimulus localization whereas the “ventral visual stream” was suggested to carry visual information to allow object recognition (Ungerleider and Mishkin, 1982). In later studies, the functions of the two streams have been expanded to the idea that the dorsal visual stream is a vision-for-action system responsible for guiding movements whereas the ventral one is involved in the perception of the objects in the visual field (Goodale and Milner, 1992; Milner and Goodale, 1995). The dorsal visual stream includes two separate channels, the dorsomedial (or dorso-dorsal) and dorsolateral one (or ventro-dorsal) which involve the SPL and IPL, respectively (Galletti et al., 2003; Rizzolatti and Matelli, 2003). It has been hypothesised that the dorsomedial stream was more implicated in the encoding of reaching movements whereas the dorsolateral one in the encoding of grasping movements (Taira et al., 1990; Jeannerod et al., 1995; Gardner et al., 2007). Despite this view is still widely accepted and also reported in neuroscience textbooks, recent studies have found in the dorsomedial visual stream not only cells with reach-related activity but also neurons activated by the orientation of the wrist and grip formation (Fattori et al., 2009, 2010) which may be recruited during prehension when a fast control mechanism is needed (Galletti et al., 2003). Therefore, currently, the two routes of dorsal visual stream are also functionally designated as “reach-to-grasp network” for the dorsomedial stream (Borra et al., 2017; Gamberini et al. ,2021) and “lateral grasping network” for the dorsolateral stream (Borra et al. 2014), considering its prevalent involvement in the control of purposeful hand actions (Figure 2).

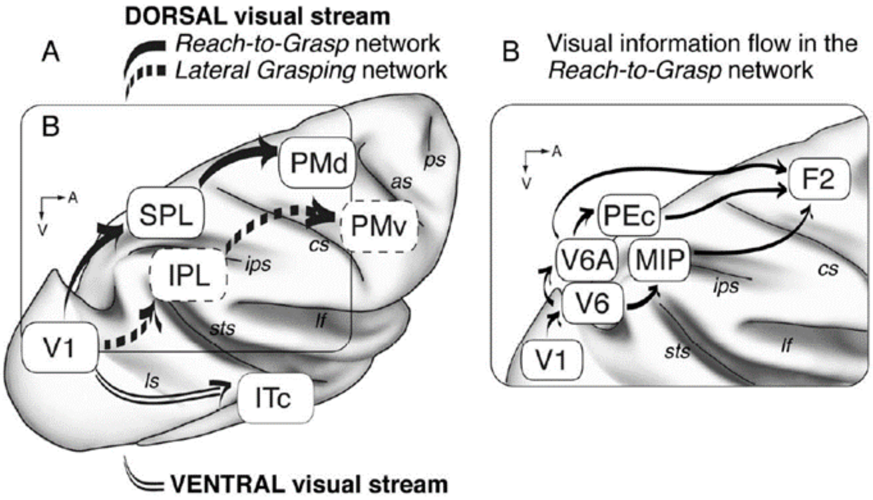

Figure 2. Dorsal and ventral visual pathway with the subdivision into the two streams; dorsomedial, the reach-to-grasp network and dorsolateral, the lateral grasping network. A*, The dorsal visual stream is organized into two main routes: in the "reach-to-grasp" network (continuous thick arrows), visual information from V1 involves parietal areas of the superior parietal lobule (SPL) and reaches the dorsal premotor areas (PMd) (Fattori et al. 2017); the "lateral grasping" network (dashed arrows) involves parietal areas of the inferior parietal lobule (IPL) and reaches the ventral premotor areas (PMv) (Borra et al. 2017). In the ventral visual stream (double continuous thin arrows), the visual information drom V1 reaches the inferior temporal cortex (ITc).* ***B****, In the "reach-to-grasp" network, visual information, starting from V1, involves areas V6, V6A, PEc and MIP and reaches the premotor area F2. Abbreviations: cs central sulcus, as arcuate sulcus, sts superior temporal sulcus, ls lunate sulcus, pos parieto-occipital sulcus, V1, V6, V6A, PEc, MIP, F2 areas V1, V6, V6A, PEc, MIP, F2, SPL superior parietal lobule, IPL inferior parietal lobule, ITc inferior temporal cortex, PMd dorsal premotor cortex, PMv ventral premotor cortex, A anterior, V ventral (Gamberini et al. 2021).*

Therefore, the suggested view is that the SPL, embedded in the dorsal visual stream, guarantees the control of all the phases of a voluntary arm-movement (Galletti et al., 2003). Noteworthy, the SPL hosts populations of neurons, in defined areas, sensitive to stimuli belonging to different sensory modalities, such as visual, motor, somatic and encode also more complex functions, such as spatial attention (Galletti et al., 2010, 1999a, 1999b)

It emerges that the SPL orchestrates these signals to realize accurate limb movements but, as a consequence, to investigate the separate contribution of each stimulus on the neural activity represent an ever relevant challenge. In the next paragraphs, I will report a descriptive overview of the neural processing of proprioception and eye signals which are crucial to monitor the arm posture during a goal-directed action.

3.2 The sense of proprioception

Sensory information about the body are elaborated continuously in the brain to decide what action to take and how to organize voluntary movements to accomplish it. Therefore, if for example we want to take a cup of tea we need to know if the cup is in a reachable position and to be aware of our arm posture all throughout the movement.

These external and internal sensory information come to the brain in form of neural signals which arise from the stimulation of specific receptors expressed in the peripheral terminals of neurons innervating the skin, muscle and joint capsules. Overall, these sensory signals travel from the sensory receptors to the spinal cord, brain stem and ultimately reach distinct areas of the cerebral cortex where information about the state of the limb are processed. Somatosensory information can be related to three main senses identified by Charles Sherrington as proprioception, exteroception, and interoception (Sherrington, 1906);

- *Proprioception*, from Latin proprius, one'own, is the sense of oneself. It enables the monitoring of posture and movements of our body parts.
- *Exteroception* is the perception of the external word mainly through the sense of touch. It is used to identify objects' properties perceiving sensations of contact, pressure, vibration, heat, cold, pain. Touch influences also how we interact with objects during active hand movement (Ryan et al., 2021).
- *Interoception* informs about the internal state of the body. Most of these sensations do not reach consciousness but are essential to regulate autonomic functions, especially in the cardiovascular, digestive, respiratory and renal systems.

The sense of proprioception relies on a series of different mechanoreceptors such as muscle spindles, Golgi tendon organs (GTO) and joint receptors, collectively referred to as *proprioceptors,* embedded in the skin, muscles, tendons, joints and ligaments.

Tactile and conscious proprioceptive information detected by the proprioceptors are transmitted to the cerebral cortex following the so called, dorsal column–medial lemniscal system. In this somatosensory pathway first-, second- and third- order neurons are involved. First-order sensory neurons have their body cell in the dorsal root ganglia adjacent to the spinal cord and project one branch of their axon to the periphery, where the stimulus is detected, and one to the spinal cord. From the spinal cord the afferents fibres ascend to the gracile nucleus (which receives signals from the upper body) and the cuneate nucleus (which receives signals from the lower body) in the medulla, and synapse on second-order neurons. Axons of second-order neurons cross over to the other side of the medulla (sensory decussation) and ascend, in the medial lemniscus, toward the thalamus, where they terminate in the ventral posterior nuclei. Finally, these nuclei convey cutaneous and proprioceptive information, at central level, to the APC which includes Brodmann's areas (BA) 3a, 3b, 1 and 2 (also referred to as the S1) and to the PPC. Moreover, APC sends projections along two parallel streams: a ventral stream, in the lateral parietal cortex (LPC), which involves the secondary somatosensory cortex (S2) and the parietal ventral area (PV), and a dorsal stream, involving part of BA5 and BA7 of the PPC (Figure 3).

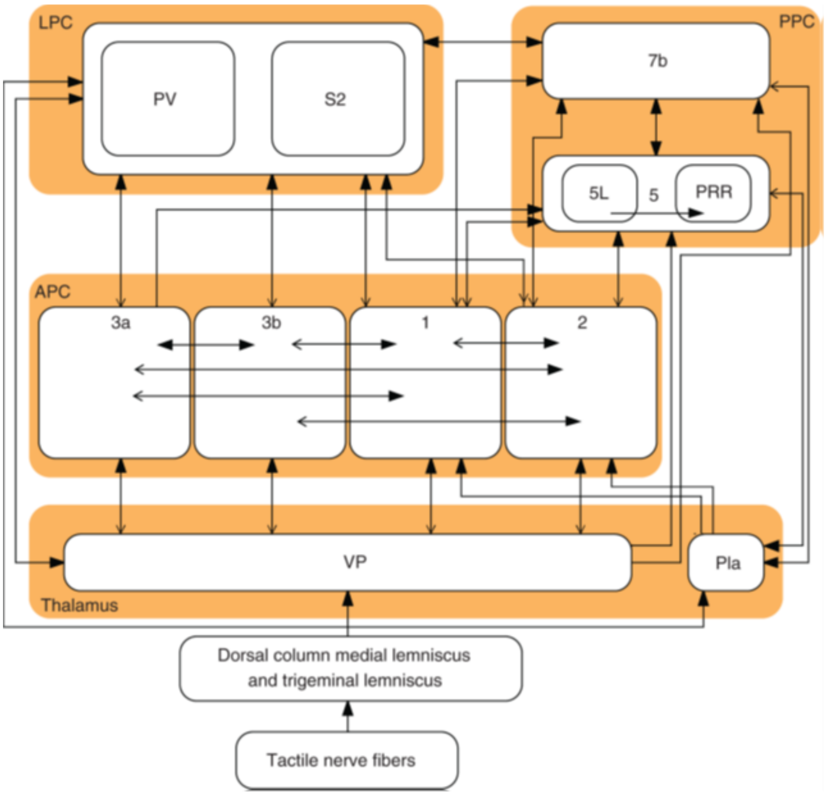

Figure 3. Major connections between areas with somatosensory properties. *Schematic representation showing connections between four major regions with somatosensory properties: the thalamus, the anterior parietal cortex (APC), the lateral parietal cortex (LPC), and the posterior parietal cortex (PPC). Abbreviations: Ventral posterior nucleus (VP), anterior pulvinar nucleus (Pla), secondary somatoensory cortex (S2), parietal ventral area (PV), parietal reach region (PRR). Area 5 also receives input from the lateral posterior nucleus in thalamus (LP, not shown in the chart; reproduced from Delhaye et al. 2018).*

The proprioceptive information is “hierarchically” processed at the central level: a result of this processing is in the complexity of receptive fields which varies across the different cytoarchitectonic areas. The large majority of cells recorded in areas 3a and 3b and many in area 1 are described as having rather “simple properties” responding to simple tactile stimuli within small cutaneous receptive fields or to movement of a joint in one direction (Powell and Mountcastle, 1959; Hyvarinen and Poranen 1978; Gardner and Costanzo 1981; Iwamura et al. 1983). Cells responding to both tactile and proprioceptive input are commonly seen in area 2 which hosts neurons responding to movement of more than one joint (Iwamura and Tanaka, 1978; Gardner and Costanzo, 1981; Iwamura et al., 1983). Area 5 receives strong input from SI (Jones and Powell, 1970; Jones et al., 1978) and these projections are highly convergent (each part of area 5 receives cortical projections from several adjacent somatotopic zones in SI (Pearson and Powell, 1985). Therefore, the somatotopic map of the body is not as fine grained in area 5 as in SI. Early single-unit recordings performed in paralyzed monkeys confirmed that many area 5 cells had more complex somatic receptive fields being optimally activated by the combinations of tactile and proprioceptive input that arose during characteristic postures (Duffy and Burchfiel, 1971; Sakata et al., 1973) (Figure 4).

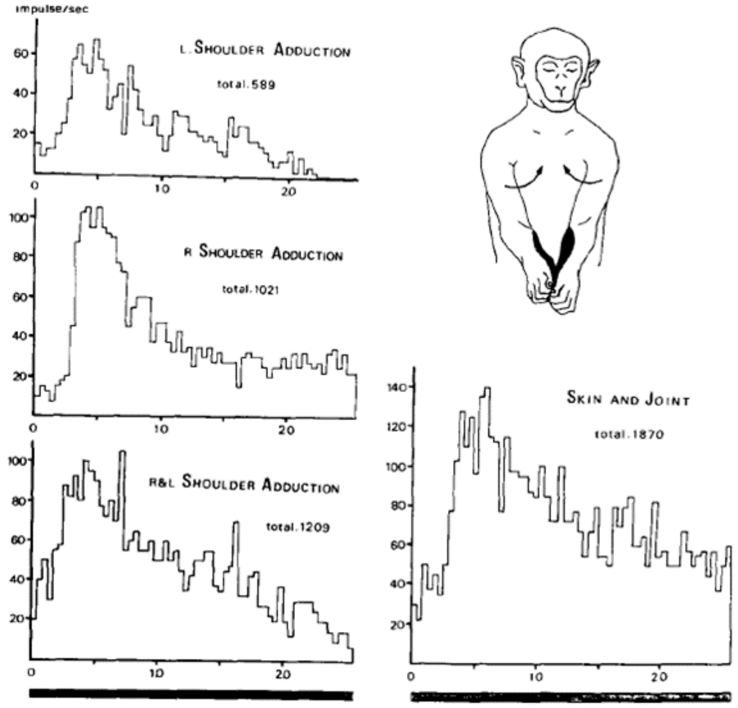

Figure 4. Response of an area 5 neuron to bilateral shoulder rotation and its enhancement by skin contact. *Left 3 PST histograms depict the responses, from above to below, to ipsilateral shoulder adduction, to contralateral shoulder adduction, and to bilateral shoulder adduction. Right histogram indicates responses to the combination of cutaneous stimulation and bilateral shoulder adduction as shown in the upper drawing. The period of stimulation is given at the bottom; the shoulder was rotated during the initial several hundred msec and then maintained in the end position (Sakata et al., 1973).*

Sakata and colleagues conclude that area 5 cells encode postures and movement patterns of whole-body segments, rather than the angle of any particular joint. Therefore, area 5 neurons represent a necessary intermediate stage in the processing of kinesthetic information, leading from a level of separate analysis of inputs from individual joints in SI to a holistic neural image of body posture and movement. One major target of area 5 output is area 7. Single cell recording experiments of Mountcastle and colleagues (1975) performed in these areas in behaving monkeys showed that some cells discharged during certain movements of the limb such as reaching to grasp pieces of fruit, or exploratory movements of the hand inside a box to retrieve a raisin (Mountcastle et al, 1975). This seminal study pointed out that area 5 has also motor properties because it contains cells activated only during active movements (11%) also represented, in higher quote, in area 7 (33%). Therefore, some parietal cells generate a somatic sensory representation of the body and others are more involved in the motor command for the movement of the arm. Overall, these somatomotor signals are likely to be used in movement guidance during purposeful actions (Mountcastle et al, 1975). In fact, a strict sensory versus motor dichotomy is too simplicistic for PPC, which is an high-order somatosensory association region.

3.3 The eye position information

As recalled above, Mountcastle and colleagues (1975) found in parietal area 7 various types of visual neurons together with movement-related neurons. They also identified visual neurons activated with ordinary visual stimuli applied in the peripheral visual field and other neurons activated during eye movements. They have been categorized into three classes: visual fixation (VF) neurons, activated by gaze position or by gaze movements, visual tracking (VT) neurons activated by smooth-pursuit tracking, and saccade-related neurons activated before and during visually-evoked saccades.

VF neurons discharged when the object of interest was in the line of gaze, and especially if it was located within arm's reach (Mountcastle et al., 1975). Sakata and colleagues (1980) challenged the idea that VF neurons where mainly related to visual attention with a role in visuospatial perception by finding a close correlation with the eye position. Noteworthy, the position of objects in the visual space cannot be determined only by retinal information, but also depends on information concerning eye position. The role of the extraretinal signals is especially important in the estimation of distance, primarily determined by the degree of convergence and accommodation (Wist, 1972).

In these experiments, Sakata recorded the activity of VF neurons in area 7a and found a modulation in their discharge according to the change in the position of the fixation point either in the radial direction, or in the distance, or both, in light and dark condition. So, the updated functional role of VF neurons was to discriminate the spatial position of a visual target and to control the direction (version) and distance (vergence) of gaze on the target (Sakata et al, 1980).

Other electrophysiological studies performed in various PPC areas found that neuronal activity was modulated by version (Andersen et al.,1990; Galletti et al., 1995; Bremmer et al., 1997; Nakamura et al., 1999) and vergence signals (Genovesio and Ferraina, 2004). The interaction between the effect of vergence and version angle across SPL areas was also investigated with an identical experimental setup with fixation points located in the 3D space, at different depths and directions (Breveglieri et al., 2012; Hadjidimitrakis et al., 2014a; Hadjidimitrakis et al., 2015; De Vitis et al., 2019).

Even though eye position effects have been demonstrated in many cortical areas, the origin of this signal is not well clarified. There are two possible sources of information about eye movement or position; one is "inflow" from proprioceptive signal of eye muscles (Sherrington, 1918) and the other is "outflow" of oculomotor signals known as corollary discharge to extraocular muscles during fixation of gaze (Von Holst, 1954). According to the inflow theory, afferent signals from peripheral transducers are the source of information about eye position and eye movement, whereas according to the outflow theory, the effective signal is derived by taking account of the muscular effort required to move the eye or hold it still.

Outflow theory is the most well accepted. Support comes from Helmholtz's (1866) observations that when the eye is passively displaced, the target rather than the eye is perceived to have moved. Moreover, when the eye is restrained during an attempted eye movement, the target is perceived to have moved in the direction of the attempted but not executed eye movement. According to these observations, the idea is that eye position compensation depends largely on outflow. In Donaldson review on the function of the proprioceptors of the eye muscles (2000) the perspective is more on considering both theories emphasizing the contribution of proprioceptive input in providing information about the position and the movement of the eye in the orbit. In addition, Donaldson discusses about the importance of proprioceptive signals from eye receptors in the normal development of visual properties of neurons in the visual cortices and for both the development and maintenance of normal visuomotor behaviour.

In the next section, I will discuss the parcellation of BA5 and BA7 of PPC of monkey brain and report the functional features of three cortical areas; V6A, PEc and PE.

3.4 Overview on Brodmann's areas 5 and 7

BA5, located on the medial side of the intraparietal sulcus (IPS), and BA7, located between the IPS and the lateral sulcus, have been divided into multiple distinct cortical fields based on cytoarchitecture, patterns of connectivity with other areas and neural response properties. BA5, originally referred to as parietal region PE (von Economo 1929; von Bonin and Bailey 1947), have been redefined and subdivided into subregions PE, PEc, PEip/ PEa, PEci (Seltzer and Pandya, 1982) and MIP (also referred to as PRR) (Colby et al., 1988). Another distinction by Lewis and Van Essen (2000) refers to two macro areas 5d and 5v.

BA7, traditionally split into a mostly somatosensory caudal area, 7a, and a mostly visual rostral area 7b (Vogt O and Vogt C, 1919) was parcellized into areas PF, PFG, PG and Opt in the surface of IPL by Pandya and Seltzer (1982) and also by Stefano Rozzi and colleagues (2006). Other cortical fields such as areas AIP and LIP lie in the lateral bank of the IPS and area VIP in the fundus of the IPS.

The anterior wall of the parieto-occipital sulcus (POs), which marks the boundary between the parietal and occipital lobe, hosts area V6A (Galletti et al., 1996 ; Galletti et al., 1999a) which borders rostrally with PEc and MIP in the medial bank of the IPS and caudally with V6, a pure visual area (Galletti et al., 1999b) (Figure 5). V6A was originally considered as part of BA19, a classical occipital area, but later studies have pointed out that it belongs to the PPC as for its cytoarchitectural pattern (Luppino et al., 2005).

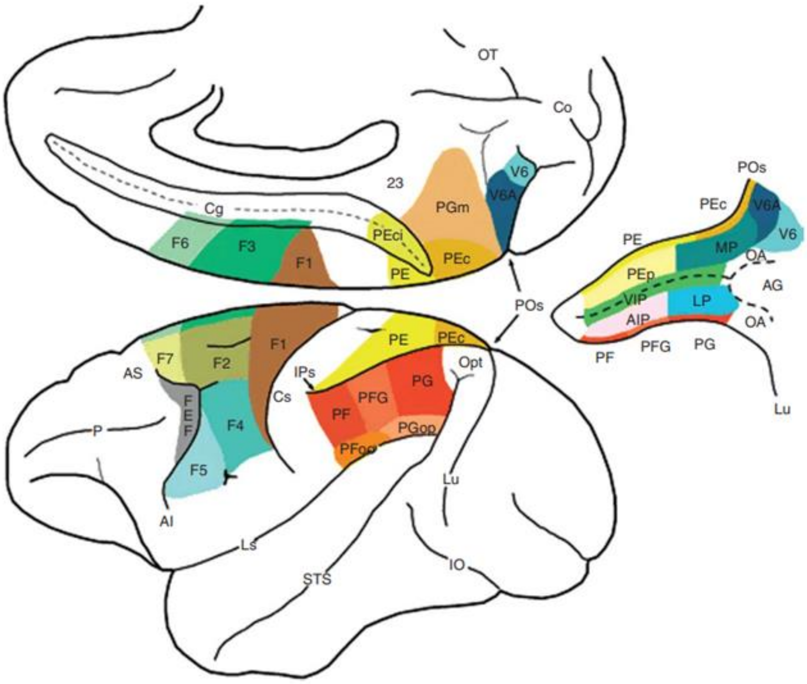

***Figure 5. Anatomical locations of frontal motor cortex areas and posterior parietal cortex areas in the macaque cerebral cortex**. Lateral and medial views of the macaque cerebral cortex showing the areas of the agranular frontal cortex according to Matelli et al. (1985, 1991) and of the posterior parietal cortex according to Pandya and Seltzer (1982). Dashed line represents the fundus of the sulcus. Abbreviations: AG annectant gyrus, AI inferior arcuate sulcus, AS superior arcuate sulcus, Ca calcarine sulcus, Cg cingulate sulcus, Cs central sulcus, IO inferior occipital sulcus, IPs intraparietal sulcus, Ls lateral sulcus, Lu lunate sulcus, OT occipitotemporal sulcus, P principal sulcus, POs parietooccipital sulcus, STS superior temporal sulcus (Reproduced from Rizzolatti and Matelli, 2003).*

Despite monkeys BA5 and BA7 are classically ascribed respectively to the SPL and IPL, recent data show that the SPL hosts both BA5 and BA7. In particular, the SPL is suggested to contain subregions PE, PEip, PEci, as part of BA5, and PEc with MIP, PGm and V6A as subregions of BA7 (Gamberini et al. 2020).

In the next paragraph, I will review the main functional properties of the SPL areas PE, PEc and V6A which are the cortical areas of interest in this thesis.

3.5 SPL areas PE, PEc and V6A

As part of the SPL, parietal areas PE, PEc and V6A integrate a multitude of stimuli related to distinct sensory modalities given their connections with other areas belonging to premotor, motor, somatosensory and visual cortices. Each area will be described below starting from its cortical connections to its respective functional properties. PE is a somatomotor area which receives projections especially from somatosensory area 2, weakly from areas 3b/S1, 1, 3a, area PEc, areas PEip, dMIP, primary motor cortex (M1/F1), medial and dorsal premotor cortex (SMA/F3, F2) (Jones and Powell, 1970; Jones et al., 1978; Strick and Kim, 1978; Zarzecki et al., 1978; Petrides and Pandya, 1984; Bakola et al., 2013) (Figure 6A). The somatosensory and motor-related information coming from these regions are likely to be integrated in PE to plan and coordinate reaching movements (Seal et al., 1985; Crammond and Kalaska, 1989; Cohen et al., 1994; Kalaska et al., 1994, 1997;

Tillery et al., 1996; De Vitis et al 2019). PE has a rough topographical map of the body containing a scarce representation of the trunk, the shoulder, multiple joints of the forelimb, multiple digits and an overrepresentation of the upper limbs in the anterolateral part (Taoka et al., 1998; Padberg et al., 2007) and of the lower ones in the posteromedial part (De Vitis et al., 2019). PE neurons are activated by proprioceptive and tactile stimuli, with most cells sensitive to joints' positions and fewer to the stimulation of the skin and responds weakly to visual input (Duffy and Burchfiel et al., 1971; Sakata et al., 1973; Mountcastle et al., 1975; De Vitis et al., 2019) (Figure 6B). Several works about the spatial effect of limb posture in the two-dimensional space showed that the neural activity in area 5 is influenced by active movements and especially by static hand positions (82% of cells activated by the maintenance of limb posture, Georgopoulos and colleagues 1984). Only few studies addressed the encoding of limb positions also in three-dimensional space demonstrating the sensitivity of PE cells to reaching movements performed at various depths and directions (Lacquaniti et al., 1995; Bhattacharyya et al., 2009; De Vitis et al., 2019)(Figure 6C). The influence of eye position in a goal-directed reaching movement was investigated only in Ferraina's study (2009), who found that a small proportion of PE neurons presents gaze direction activity (13%) whereas the majority (61%) is modulated by the position of the hand.

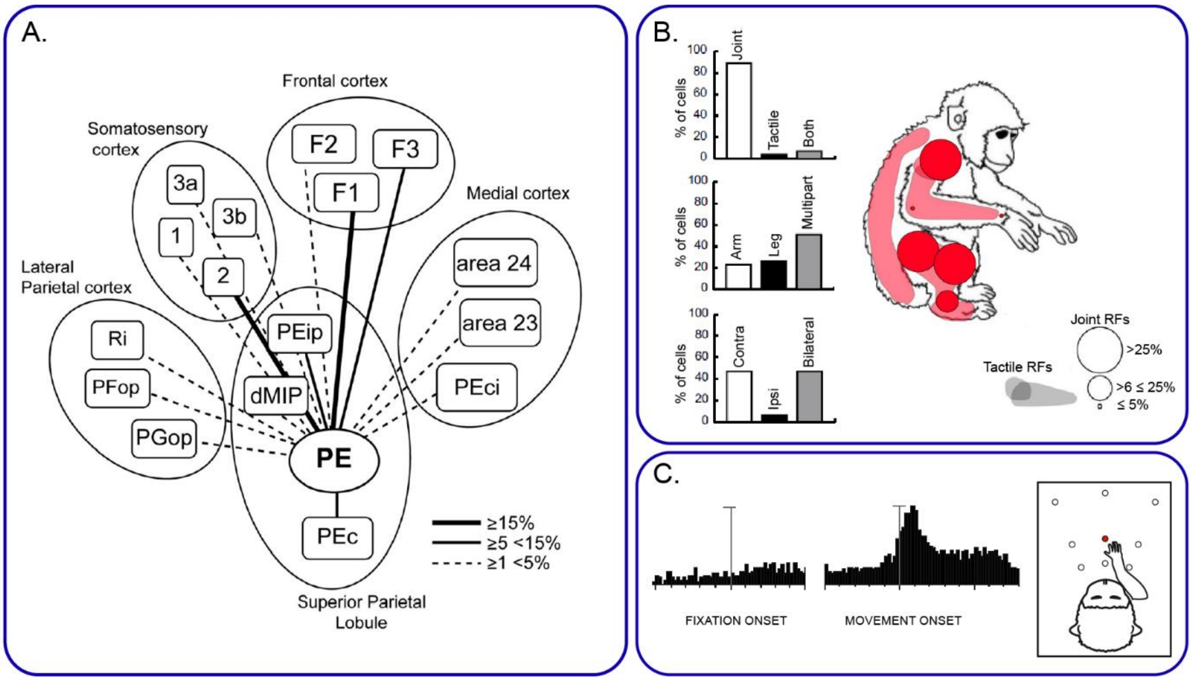

Figure 6. Schematic map with projections to area PE and summary of sensory and motor properties. ***A****, Summary of cortical connections of area PE. The boxes representing different areas are organized approximately in a caudal to rostral sequence, from the bottom part of the figure to the top. The thickness of the bars shows the proportion of cells in each of the areas connecting with PE (modified from Bakola et al., 2013).* ***B****, PE cells with somatosensory properties and locations of somatosensory receptive fields. Histograms show from the top to the bottom the incidence of cells responsive to different somatosensory submodalities, the incidence of body part representation and of laterality of somatosensory responses. In the right side of the panel there is an illustration of body locations of somatosensory (red patches) and joints (red circles) reference frames (RFs) in PE. All RFs have been reported on the animal's right side (modified from De Vitis et al., 2019).* ***C****, Example of a PE cell of a Macaca monkey sensitive to the arm movement. The cell activity is illustrated as a peri-event time histogram aligned at the fixation and movement onset (vertical bars) and corresponds to the movement executed to reach one of nine targets (red circle) located in a horizontal panel, placed at the animal eye level (modified from De Vitis et al., 2019).*

Located caudally to PE, PEc was originally described by Pandya and Seltzer (1982) as a somatosensory association area of BA5. It is currently considered a visuomotor area, more likely to be part of BA7 (Luppino et al., 2005, Gamberini et al., 2018, 2020). Beside the strong connections with somatosensory-related cortex as PE and PEci, this area receives also motor projections from area F2, weakly from areas F3, F1 and is connected with visuomotor areas dMIP and dV6A (Bakola et al., 2010) (Figure 7A, PEc). PEc does not show a somatotopic organization but the representation of the body is quite complete.

Most PEc somatosensory cells respond to passive rotation of limb joints (73%) whereas a minor quote is responsive to tactile stimulation (27%). Tactile receptive fields are located mainly on the arm (61%) but they are also present in the trunk and the leg (22% and 17% respectively) (Breveglieri et al., 2006) (Figure 7B, PEc). PEc neurons are activated by arm-reaching movements and are sensitive to oculomotor, eye position and visual signals (Batista et al., 1999; Battaglia-Mayer et al., 2001; Ferraina et al., 2001; Breveglieri et al., 2006, 2008) (Figure 8A, PEc). Noteworthy, this area receives projections from areas MIP and V6A which are directly connected with visual area V6 and are likely to distribute visual and eye positions information to PEc.

In PEc, with respect to PE, somatosensory cells are less represented and mainly activated by single rather than multiple joints signals. PEc contains also bimodal cells, neurons that process more than one sensory input, sensitive to both somatosensory and visual stimuli, not present in PE (Breveglieri et al., 2008).

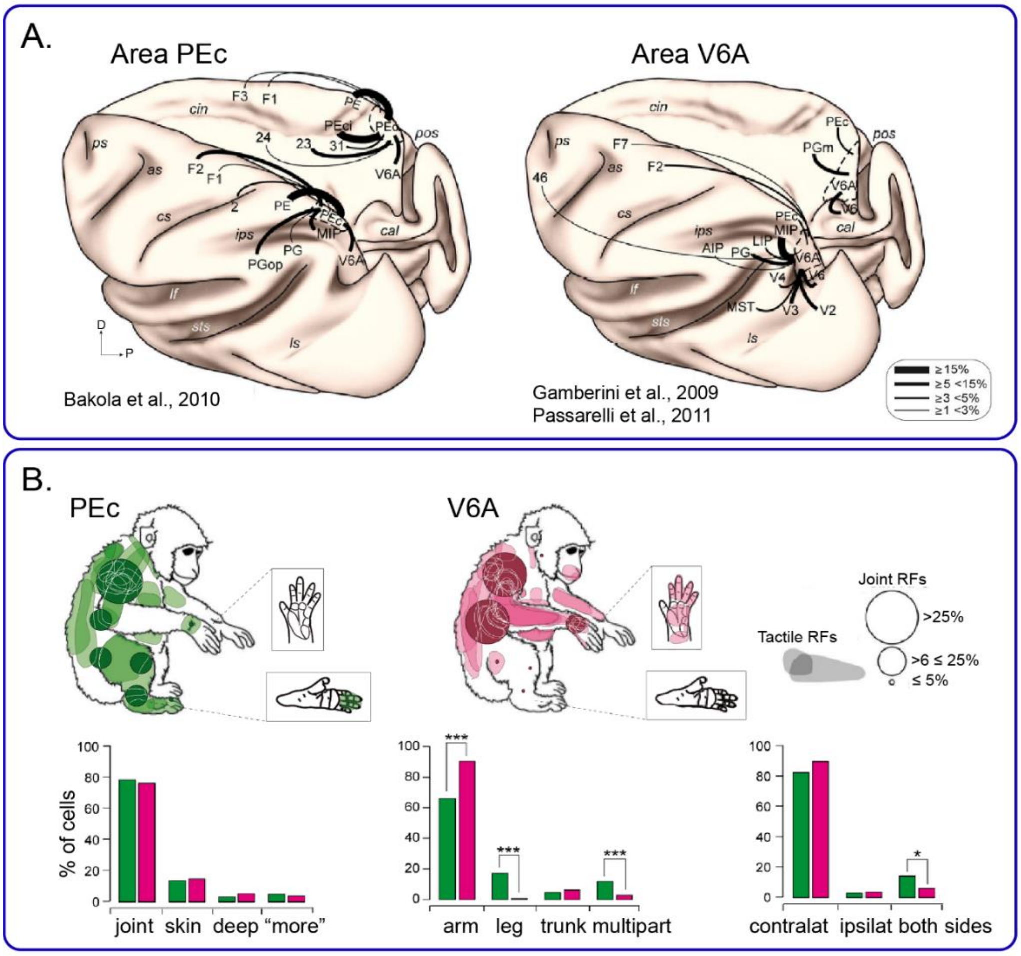

Figure 7. Main cortico-cortical connections of areas PEc and V6A and somatosensory properties. A*, For each area, only projections representing more than 1% of the total cortical connections of that area are reported. The thickness of connecting lines is proportional to the strength of connections, as indicated in the legend within the figure. Abbreviations: D dorsal, P posterior; F1, F2, F3, F7, 23, 24, 31, PEci, PE, PEc, PGm, V6A, PGop, PG, MIP,46, AIP, LIP, VIP, V2, V3, V4,V6, MST: areas F1, F2, F3, F7, 23, 24, 31, PEci, PE, PEc, V6A, PGop, PG, MIP,46, AIP, LIP, VIP, V2, V3, V4,V6, MST; as arcuate sulcus, cs central sulcus, lf lateral fissure, ls lunate sulcus, sts superior temporal sulcus, ips intraparietal sulcus, cin cingulate sulcus, ps principal sulcus, pos parieto-occipital sulcus (modified from Gamberini et al. 2020).* ***B****, Somatosensory properties of PEc (green) and V6A (magenta) cells and locations of somatosensory receptive fields. Top, locations of somatosensory RFs in PEc and V6A: joints RFs are indicated as dots whose size is proportional to the number of modulated units, and tactile RFs as colored patches whose color intensity is proportional to the number of overlapped RFs. All the RFs have been reported on the animal's right side. RFs reported on the left arm represent RFs located on the internal part of the arm (not visible if drawn on the right arm). Boxes to the right of monkey's silhouettes report close-up view of the hand and foot. Bottom histograms show from left to right the incidence of cells responsive to different submodalities of somatosensory responses; "more" are cells driven by more than one type of stimulation (i.e., joint and deep stimuli), the incidence of body part representation and of laterality of somatosensory responses. The results of χ2 test are indicated by asterisks, ***$p < 0.005$;*$p < 0.05$ (modified from Gamberini et al. 2018).*

Area V6A borders rostrally with PEc and lies in the anterior bank of the POs (Galletti et al., 1999a, 1999b) (Figure 7A, V6A). It is subdivided into a dorsal and ventral cytoarchitectonic field, named V6Ad and V6Av (Luppino et al., 2005). V6Ad, which is connected mainly with parietal (MIP, PEc, PGm, LIP, VIP, AIP, PG, and Opt) and frontal cortices (premotor area F2, F7 and weakly with prefrontal area 46) has visuomotor properties whereas V6Av, which receives strong inputs from visual (V2, V3, V4, V6, and MST) and parietal (PGm, V6Ad, and MIP) cortices, is primarily considered a visual area that brings visual information from V6 to V6Ad (Gamberini et al., 2009 ; Passarelli et al., 2011). Although both areas V6Av and V6Ad are not retinotopically organized, V6Av mainly represents the peripheral part of the visual field while V6Ad the central part of it. In V6A visual neurons are more common with respect to somatosensory neurons and, as PEc, also this area contains bimodal cells (Gamberini et al., 2018). The somatotopic representation in V6A is limited only to the upper limbs with respect to PEc which contains both the upper and lower limbs (Breveglieri et al 2002; Gamberini et al., 2011) (Figure 7B, V6A). V6A neurons are involved in reaching, grasping, and ocular movements (Galletti et al., 1995; Fattori et al., 2001, 2005, 2009, 2010; Kutz et al., 2003) (Figure 8B, V6A) and are modulated by spatial attention (Galletti et al., 1996, Galletti et al., 2010).

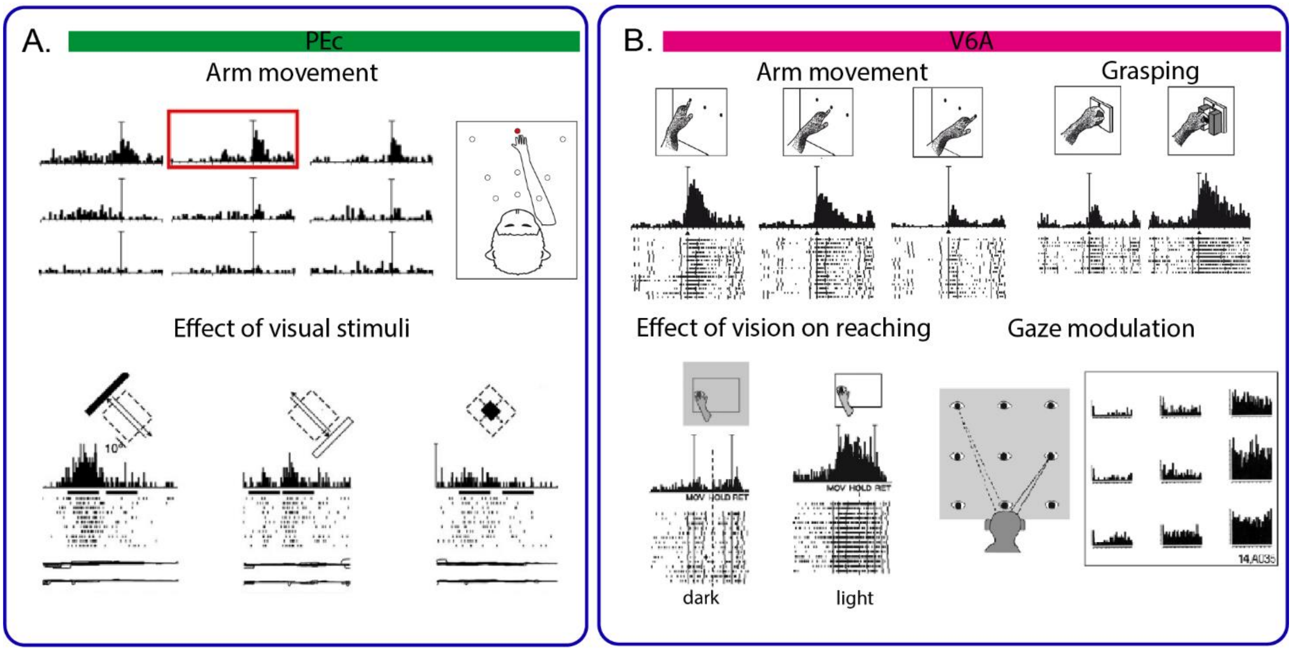

Figure 8. Example of PEc and V6A cells sensitive to movements and visual stimuli. ***A****, Top: activity of a PEc neuron spatially modulated for Far target positions during the movement phase of a reaching task. The activity is represented as peristimulus time histograms (PSTH) for each of the nine reaching target positions located at three directions (columns) and depths (rows). On the right, schematic representation of the task with reaching targets (circles) located in a horizontal panel at monkey eye level. The corresponding neural activity for the red target illustrated is evidenced with a red rectangle. Vertical lines indicate the alignment of activity at the arm movement onset (modified from Piserchia et al., 2017). Bottom: responses of a PEc cell represented as PSTH and raster dot displays to a moving dark bar, to moving light bar, and to expanding—contracting dark square (modified from Breveglieri et al. 2008).* ***B****, Top: responses of two V6A neurons. From left to right, a cell activated by the direction of arm reaching movement and a neuron sensitive to the grip type with a higher activity during a precision grip. Bottom: from left to right, a V6A reaching neuron strongly responsive in the light, but not in the dark and a V6A neuron modulated by the direction of gaze. The animal sat in front of a vertical screen while fixating different screen positions. The activity of the cell is shown as PSTH located on the screen in the positions fixated by the animal and it is aligned at the fixation onset (modified from Galletti et al. 2022).*

Despite the common role of the three SPL areas in goal-directed actions, the proposed view is that V6A and PEc are both visuomotor areas which share similar functional features and process complex sensory input, whereas PE is a somatomotor area more involved in elaborating somatosensory signals.

Up to date, a direct comparison of these SPL areas in the encoding of the direction of gaze and proprioceptive signals of the limb at the end of a reaching movement in the three-dimensional space is still lacking. Therefore, the purpose of this thesis is to investigate whether a different level of integration of these signals is operated in the SPL and find a possible parallel with the functional similarities descripted above between caudal areas V6A and PEc and rostral area PE.

Moreover, the results could support the recent idea that V6A and PEc have more in common, also from a structural point of view, as part of BA7 with respect to PE which belongs to BA5 (Gamberini et al., 2020).

4. AIM OF THE THESIS

During a voluntary arm movement the eyes are constantly kept on the desired target, whereas the limb posture changes until the arm is held in a steady position, at the end of the reaching action. Therefore, eye and limb positions signals are elaborated in the brain to ensure the maintenance of the arm in the correct spatial location. As summarized before, areas V6A, PEc and PE of the SPL are notoriously engaged in the control of reaching movements; V6A and PEc are visuomotor areas which contain cells with somatosensory, visual, bimodal (somato-visual), motor and oculomotor properties, whereas PE is a somatomotor area rich in cells sensitive to somatosensory stimuli and movement-related ones. These areas use all these information for reaching control but the degree of independent encoding of these signals is still under debate. The aim of this thesis is thus to investigate how V6A, PEc and PE combine gaze and proprioceptive information at the end of a movement in the three-dimensional space. Then, we wondered whether the processing of eye and limb positions signals parallels the functional gradient present in the SPL with the caudal sectors more influenced by vision and somatosensory stimulations and the rostral sector by proprioception. Finally, we investigated whether the different level of encoding in these areas overlaps also the subdivision of V6A and PEc in BA7 and of PE in BA5 in the monkey brain as proposed by Gamberini and colleagues (2020).

5. MATERIALS AND METHODS

5.1 Experimental procedures

Two male macaque monkeys (*Macaca fascicularis*), weighing 4 and 4.6 kg, were involved in this study. The experiments were performed in accordance with the guidelines of EU Directives (86/609/EEC; 2010/63/EU) and Italian national laws (D.L.116–92, D.L. 26–2014) on the protection of animals used for scientific purposes. Protocols were approved by the Animal-Welfare Body and from the Italian Ministry of Health. During training and recording sessions, particular attention was paid to any behavioural and clinical signs of pain or distress.

5.2 The Fixation-to-Reach task

The animal sat in a primate chair (Crist Instruments) and performed a Fixation-to-Reach task. During this task, the monkey sat in front of a horizontal panel located at eye level with nine light-emitting diodes (LEDs; 6 mm in diameter) placed at different distances and directions used as fixation and reaching targets (Figure 9). Since the targets were aligned at eye level, they could potentially obscure each other. We got the problem solved by gradually masking the LEDs, going from the thinner nearest targets to the ticker farthest one. Thus, the monkeys were able to easily discriminate them. The task was performed in darkness with the hand contralateral to the recording site. In the starting position, the monkey kept its hand on a button [hereafter called the home button (HB), 2.5cm in diameter] placed 4 cm in front of the chest, outside the animal's field of view (Figure 9). Target LEDs were arranged in three rows: one central, along the sagittal midline, and two laterals, at version angles of -15° and +15°, respectively. Along each row, three LEDs were located at different depth, at vergence angles of 17.1°, 11.4°, 6.9°. The nearest targets were located at 10 cm from the eyes, whereas the LEDs placed at intermediate and far positions were located at 15 and 25 cm, respectively (Figure 9). Target positions were chosen to be all within the peripersonal space.

A trial began when the monkey pressed the HB (Figure 9, HB press). After 1 s, one of the nine LEDs was switched on to green and the monkey had to fixate the LED while keeping the HB button pressed (Figure 9, LEDon). Then, the monkey had to wait 1.5–2.5 s for a change in the color of the same LED (from green to red) without performing any eye or arm movement (Figure 9, epoch FIX). The color change was the go signal for the animal to release the HB and start an arm movement toward the target. Once reached the target, the animal was required to hold the hand on it for 0.8–1.2 s (Figure 9, epoch HOLD). Target switching off cued the monkey to release it and return to the HB, which ended the trial and allowed the monkey to receive its reward. Note that during FIX the monkey maintained the gaze still on one of the nine LEDs while the arm was located near the body because the hand was pressing the HB; during HOLD, the animal maintained fixation on the target LED while pushing it, so the arm was extended and motionless, and the hand was far from the body.

Stimuli presentation and animals' performance were monitored using custom software written in Labview (National Instruments), as described previously (Kutz et al., 2005); if monkey broke fixation, made an incorrect arm movement, or did not respect the temporal constraints of the task, the trial was aborted. Microswitches (monopolar microswitches, RS Components) were mounted under the HB and under each LED to monitor the correct performance of arm movements. Eye position signals were sampled with two cameras (one for each eye) of an infrared eye-tracking system (ISCAN) at 100 Hz and were controlled by an electronic window (4°x 4°) centred on the fixation target. If the monkey fixated outside this window, the trial was aborted. The task was performed in darkness, in blocks of 90 randomized trials, 10 for each LED target position.

At the beginning of each recording session, the monkey was required to perform a calibration task to calibrate the eye tracker. In this task, animal fixated 10 LEDs mounted on a frontal panel at 15 cm from the eyes. For each eye, signals to be used for calibration were extracted during the fixation of five LEDs, one central aligned with the eye's straight-ahead position, and four peripheral ones placed at an angle of ±15° (distance: 4 cm) both in the horizontal and vertical axes. From the two individual calibrated eye position signals, we derived the mean of the two eyes (the conjugate or version signal), and the difference between the two eyes (the disconjugate or vergence signal) using the equations: Version = (R + L) ÷ 2 and Vergence = L - R, where R and L were the position of the right and left eye, respectively, expressed in degrees. The version and vergence values were also used by the LabVIEW software to control the gaze position and abort trials in case of incorrectness.

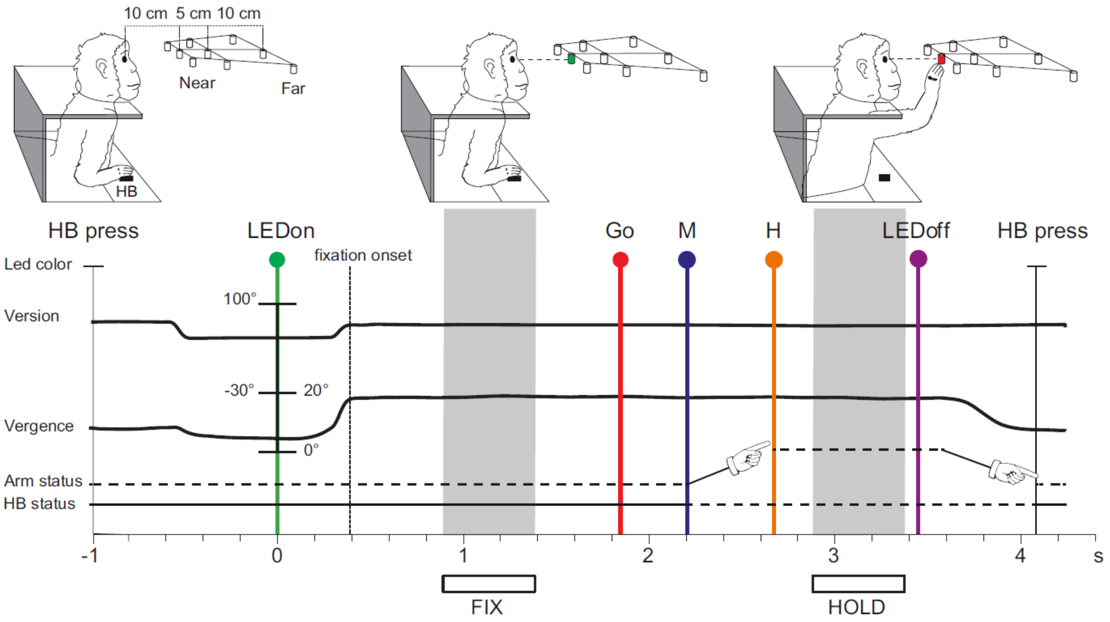

Figure 9. Scheme of the experimental setup and timing of the task. *The monkey sat in a primate chair in front of a horizontal panel located at eye level with nine LEDs used both as fixation and reaching targets. HB, home button. The distances in depth between the three targets of the central row from mid-eye level are shown. The time sequence of task events shows LED status, the eye's vergence and version traces, arm status, and HB status. From left to right, vertical lines indicate, respectively, trial start (HB press, black line), target appearance (LEDon, green line), fixation onset (end of saccade movement, dashed line), go signal (Go, red line), arm movement onset (M, blue line), holding phase of the target (H, orange line), turning off of the LED (LEDoff, purple line), and trial end (HB press, gray line). Arm drawings indicate the forward and backward arm movement. The relevant time intervals (epochs) used for the analysis of neural activity are indicated with gray areas and white bars below the time axis: FIX = fixation epoch, HOLD =holding epoch.*

5.3 Surgical and recording procedures

After training completion, a head-restraint system and a recording chamber were surgically implanted in asepsis and under general anesthesia (sodium thiopental, 8 mg/ kg/h, i.v.) following the procedures reported in Galletti et al. (1995). Adequate measures were taken to minimize pain or discomfort. A full program of postoperative analgesia (ketorolac trometazyn, 1 mg/kg, i.m., immediately after surgery, and 1.6 mg/kg, i.m., on the following days) and antibiotic care [Ritardomicina® (benzathine benzylpenicillin + dihydrostreptomycin + streptomycin) 1–1.5 ml/10 kg every 5–6 d] followed the surgery. Single-cell activity was extracellularly recorded from areas V6A, PEc, and PE of the two monkeys. We performed single microelectrode penetrations using a 5-channel multielectrode recording system (MiniMatrix, Thomas Recording, GmbH). The electrode signals were amplified (at a gain of 10,000) and bandpass filtered (between

0.5 and 5 kHz). Action potentials in each channel were isolated online with a waveform discriminator (Multi Spike Detector; Alpha Omega Engineering). Spikes were sampled at 100 kHz. The present study includes neurons assigned to areas V6A, PEc, and PE following the cytoarchitectonic criteria of Pandya and Seltzer (1982) and Luppino et al. (2005) (recording regions are depicted in Figure 10).

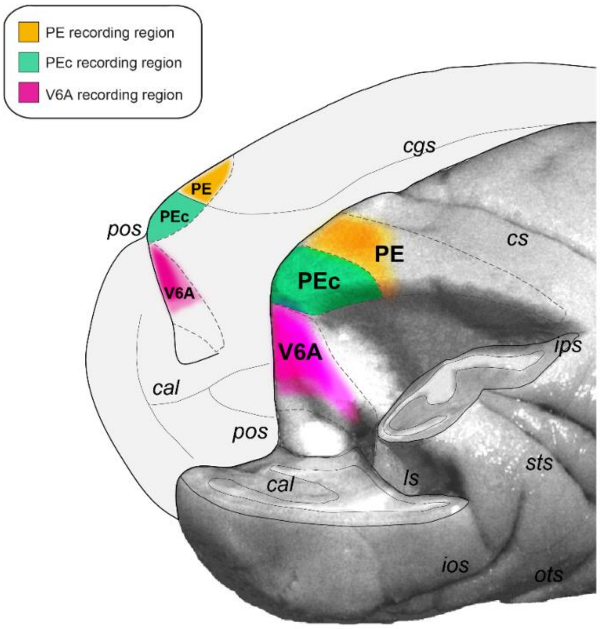

Figure 10. Areas of the superior parietal lobule in a macaque brain. *Posterolateral view of a part of M. fascicularis brain showing location and extent of areas V6A, PEc, and PE (outlined by gray dashed lines) of the SPL. The right hemisphere is partially dissected to show the areas hidden in the parieto-occipital and intraparietal sulci. Colored areas represent the reconstructions of the recording regions within these areas as a mean of two animals and four hemispheres. cal, calcarine sulcus; cgs, cingulate sulcus; cs, central sulcus; ios, inferior occipital sulcus; ips, intraparietal sulcus; ls, lunate sulcus; ots, occipitotemporal sulcus; pos, parieto-occipital sulcus; sts, superior temporal sulcus (modified from Gamberini et al., 2020).*

5.4 Data analysis

All the analyses were performed using custom scripts in MATLAB (MathWorks, RRID: SCR_001622). Analysis of the neuronal activity during the Fixation-to-Reach task was made by quantifying the discharge recorded during each trial in the following time epochs (Figure 9):

- FIX: from 500 ms after fixation onset (corresponding to the onset of ocular fixation inside the electronic window) until 1000 ms after it. It contains the neural discharge for LED fixation, avoiding transient saccade-related responses (see Kutz et al., 2003).

- HOLD: from 200 ms after LED pressing until 700 ms after it. It contains the discharge of the cells during hand holding, avoiding transient responses related to the stop of the arm movement.

We included in the analyses only those units recorded during at least seven trials per spatial position, and with a mean firing rate in HOLD and/or in FIX higher than three spikes/s in at least one position. The reasons for these conservative criteria are dictated by the intrinsic high variability of biological responses in the PPC as explained in detail in Kutz et al. (2003).

To assess the effect of the eye and arm position on V6A, PEc, and PE cells, we performed a two-way ANOVA with factors being the epoch (two levels: FIX and HOLD) and target positions (nine levels: nine spatial positions of the reaching targets). FIX was chosen as a reference because in this epoch the gaze was still, and the monkeys were not required to execute any arm movement. We defined as task-related and further analyzed those cells showing significant main effects of both target positions and epoch ($p < 0.05$), significant interaction (target positions*epoch, $p < 0.05$), or a cumulative main and interaction effect (epoch+interaction, target positions+interaction).

Significant modulation of neural activity by the target position in each epoch of interest was assessed by a oneway ANOVA (factor: target position, $p < 0.05$). The incidence of task-related cells with significant modulations by the target position during HOLD, FIX and both FIX&HOLD epochs was compared in the three areas V6A, PEc, PE with a z-test (Zar, 1999), as detailed in Fluet et al. (2010).

To perform this test, the SE of the sampling distribution difference between two proportions was computed as:

$$SE = \sqrt{p(1-p)[(1 \div n1)(1 \div n2)]}$$

with $p = [(n1 \times p1)(n2 \times p2)] \div (n1 + n2)$ representing the pooled sample proportion and $n1 \div p1$ and $n2 \div p2$ representing the size and proportion, respectively, of each sample. Subsequently, the z score was calculated as $z = (p1 - p2) \div \mathrm{SE}$, and its corresponding p value was obtained from the (cumulative) normal distribution.

A z-test was also used to compare the incidence of task-related cells with higher firing rate during HOLD with respect to FIX in all the nine positions (referred as excited cells) and with lower firing rate during HOLD with respect to FIX in all the nine positions (referred as inhibited cells).

To analyze the spatial tuning of task related cells activity during the time-course of the task, a stepwise multiple linear regression model was applied with a sliding window approach (window-bin width: 250 ms; step: 50 ms). A similar method has been used in previous publications from our lab (Hadjidimitrakis et al., 2014a, 2015; De Vitis et al., 2019). To dynamically relate the neural activity to the different target positions over time, we applied the following equation for the firing rate using this regression model:

$$A(Xi, Yi) = b0 + b1Xi + b2Yi$$

where A was the neural activity in spikes per second for the ith trials; Xi and Yi the positions of the target defined as vergence and version angles, respectively, of the eyes; b1 and b2 were regression coefficients and b0 the intercept. After being tested for their significance, the vergence and version coefficients were normalized with the standard deviation of vergence and version, correspondingly. In each bin, the sign of the significant linear correlation coefficients was used to determine the spatial preference per each neuron.

Population responses of neurons modulated by the target position during HOLD and FIX&HOLD epochs were computed as averaged spike density functions (SDFs). An SDF was calculated (Gaussian kernel, half-width 40ms) for each neuron included in the analysis and averaged across all the trials for each target position. The peak discharge of the neuron found over all the nine target positions during the epoch of interest (HOLD or FIX) was used to normalize all the SDFs. The normalized SDFs were then averaged to obtain population responses (Marzocchi et al., 2008). To statistically compare the population SDFs curves of best and worst positions SDFs in each area, we performed a permutation test (10,000 iterations), comparing the sum of squared errors of the actual and randomly permuted data. Comparisons of responses to target fixation have been made in the interval from 500 ms to 1000 ms after saccade offset for FIX. Comparisons of responses related to static positions of the arm have been made in the interval from 200 ms after the LED pressing till 700 ms after it for HOLD. The onset of spatial selectivity was calculated as the time of divergence of population SDFs of the best and worst target position (half-Gaussian kernel, width 5ms).

6. RESULTS

We have investigated the influence of gaze and arm proprioceptive signals on the activity of neurons of 3 SPL areas (V6A, PEc, PE) in two macaque monkeys. Animals performed a Fixation-to-Reach task being instructed to fixate and reach nine foveated targets located at different spatial locations in the 3D space facing the animal (Figure 9). Only the horizontal plane at eye level was explored to reduce the factors influencing neuronal activity, being well known that gaze elevation modulates the activity of neurons in the caudal part of SPL (Galletti et al., 1995; Breveglieri et al., 2012). The task allowed us to test the influence of gazing different positions of the peripersonal space (epoch FIX) and of holding the arm in different spatial configurations (epoch HOLD) on neuronal activity.

We recorded the activity of 303 single V6A cells (Left Hemisphere: 218, Right Hemisphere: 85; Monkey A: 168, Monkey B: 135), 264 PEc cells (Left Hemisphere: 159, Right Hemisphere: 105; Monkey A: 157, Monkey B: 107), and 189 PE cells (Left Hemisphere: 91, Right Hemisphere: 98; Monkey A: 69, Monkey B: 120). We analyzed neural responses during two epochs: target fixation (FIX, from 500 ms after fixation onset till 1000 ms after it, Figure 9) and target holding (HOLD, from 200 ms after the LED pressing till 700 ms after it, Figure 9).

6.1 Effect of Eye and Arm Position Signals on V6A, PEc and PE

We examined how many V6A, PEc, and PE neurons were significantly modulated by the eye and arm position (two-way ANOVA, $p < 0.05$) and identified them as “task-related”. A total of 226/303 V6A cells (75%), 188/264 PEc cells (71%), and 85/189 PE cells (45%) showed task-related activity and were further analyzed. Figures 11-13 show three examples of neurons modulated during the Fixation-to-Reach task, recorded from the areas V6A, PEc, and PE, respectively. Task-related V6A neuron showed in Figure 11 was modulated by the spatial position of reaching target both in FIX (one-way ANOVA, $p=3 \times 10^{-5}$) and HOLD (one-way ANOVA, $p=3 \times 10^{-8}$) and showed a higher discharge during HOLD for far targets, mainly the ipsilateral one. This cell displayed low activity during arm movement and peaked in discharge after the target LED pressing, when the monkey's arm was still and extended (HOLD). Task-related PEc neuron showed in Figure 12 exhibited a spatial preference for positions ipsilateral and near the body (one-way ANOVA, $p = 0.001$ during FIX, $p=10^{-6}$ during HOLD). Cell's activity gradually increased after the go signal, peaked around the target LED pressing, and decreased afterward, but remained quite high during the HOLD epoch. In contrast to V6A, PE neuron discharged strongly during arm movement (Figure 13). Its activity was modulated by the spatial position of the arm during HOLD (one-way ANOVA, $p=5 \times 10^{-5}$), whereas the activity during FIX was comparable in the nine target positions ($p = 0.05$).

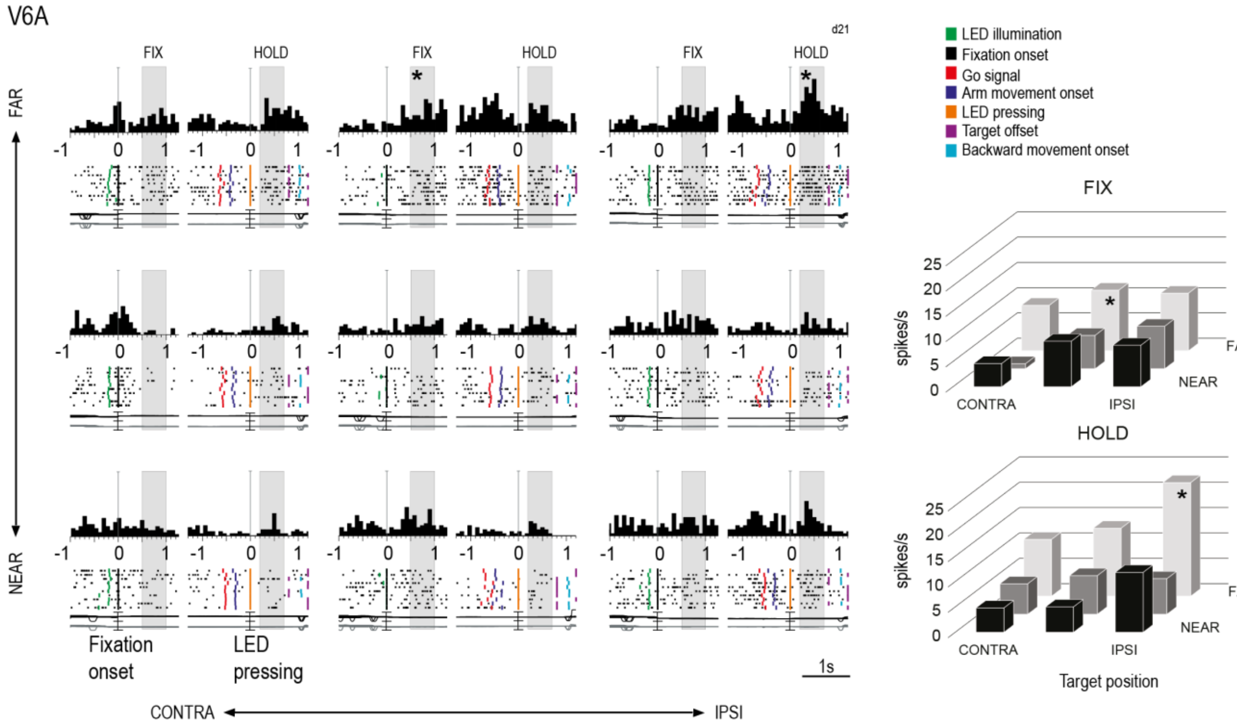

***Figure 11. Example V6A neuron tuned by eye/arm positions both in FIX and HOLD. Left**, Spike histograms (top), rasters (middle), eye traces (bottom) are shown for each of the nine target positions tested. Target positions were arranged in three directions (columns; contralateral, central, ipsilateral with respect to the recording hemisphere) and three depths (rows; far, intermediate, near with respect to the monkey's body). Colored vertical lines along rasters indicate behavioral markers that, from left to right, are: LED illumination, fixation onset, go signal, movement onset, movement end (LED pressing), target offset, backward movement onset. Thin vertical lines along spike histograms indicate the alignment of activity at the fixation onset and LED pressing, respectively. Realignment is evidenced with a gap in histograms. Epochs of interest are represented within gray rectangles. Vertical scale on histograms: 40 spikes/s. **Right**, Distribution of the mean activity of the same cell across trials during epochs FIX (top) and HOLD (bottom) for each of the nine target positions tested. Asterisks indicate the spatial position evoking the highest discharge in each epoch.*

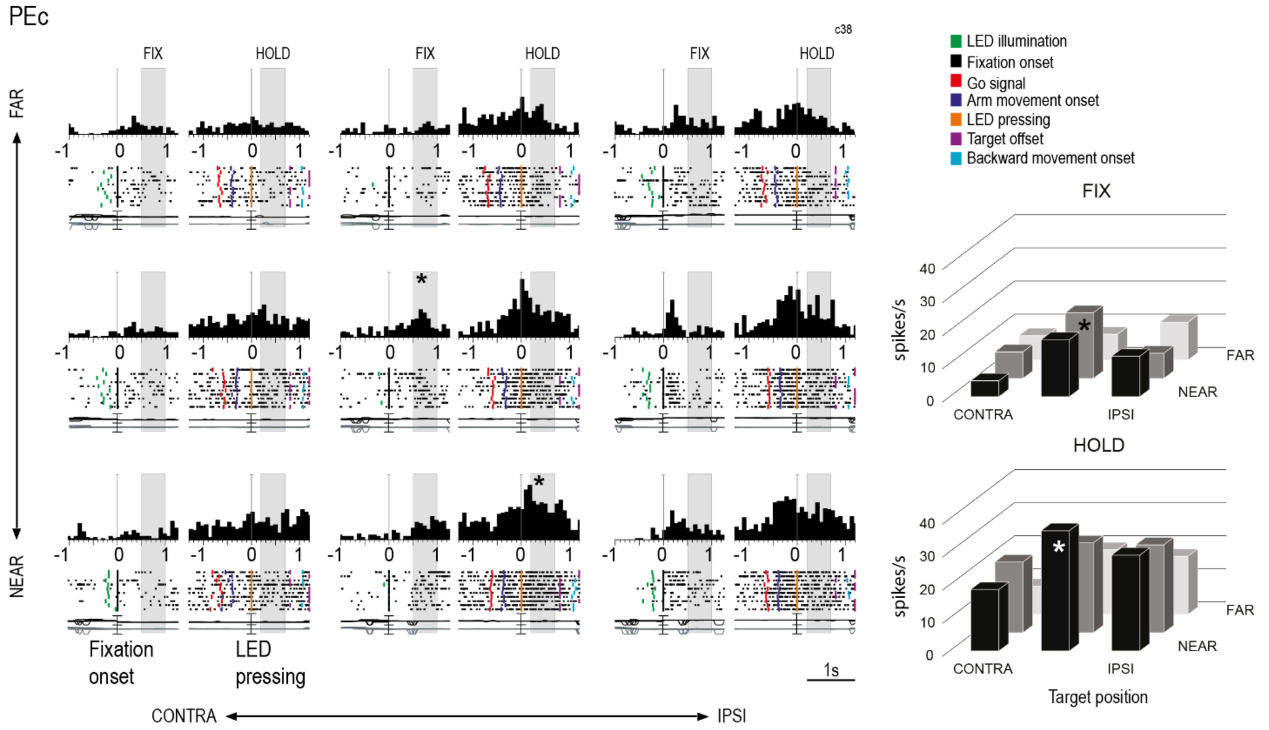

***Figure 12. Example PEc neuron tuned by eye/arm positions both in FIX and HOLD**. All the conventions as in Figure 11. Vertical scale on histograms: 70 spikes/s.*

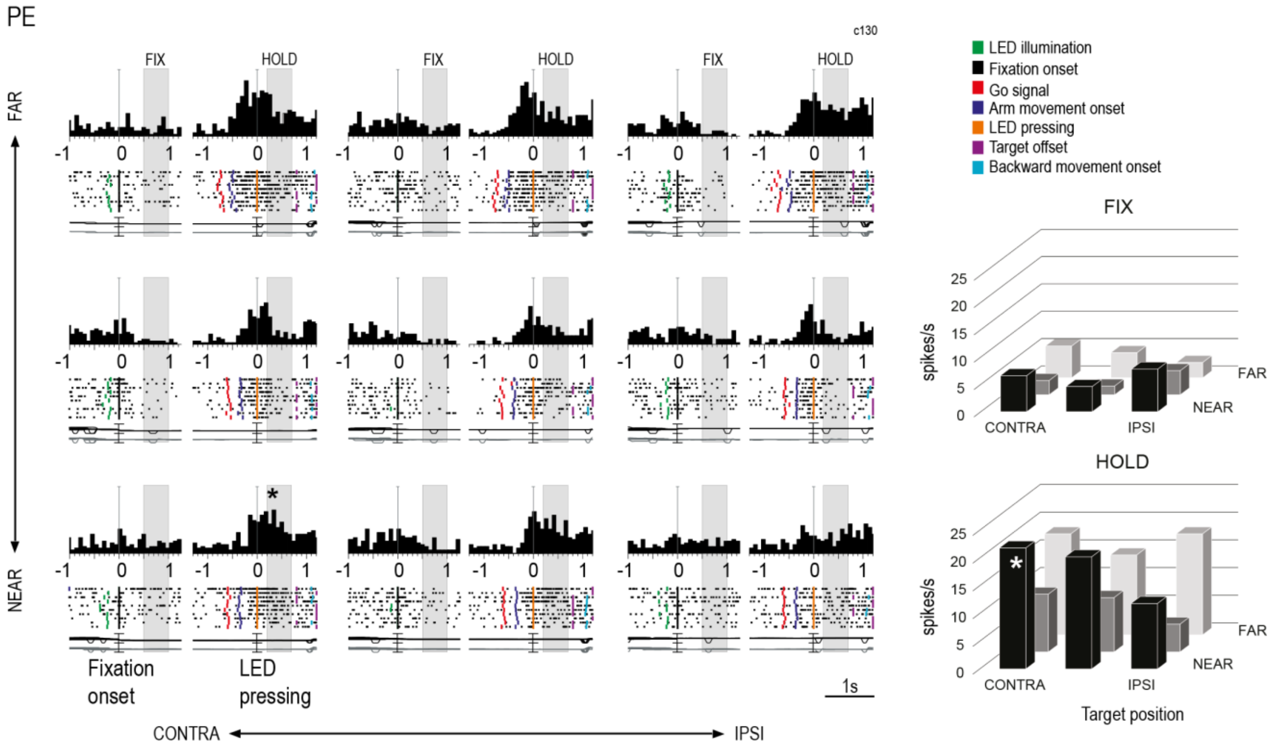

***Figure 13. Example PE neuron tuned by eye/arm positions only in HOLD.** All the conventions as in Figure 11. Vertical scale on histograms: 48 spikes/s.*

Different functional features were observed in PE on one side and in PEc/V6A on the other: firstly, a lower incidence of task-related cells was found in PE compared with both PEc and V6A (z-test, PE vs PEc $p=2 \times 10^{-8}$, PE vs V6A p=5 x 10^{-6}), whereas no significant difference was found between V6A and PEc (z-test, p = 0.4). We categorized neurons in four classes, according to their modulation by fixation and arm holding in space (epoch, EPO in Figure 14A) and by the nine spatial positions (target positions, POS in Fig. 13A) during one or both the epochs of interest. Therefore, we distinguished: (1) neurons significantly modulated by the eye position, the arm position in space, or by both (POS+EPO; Figure 14A); (2) neurons modulated only by the interaction POS*EPO (INT; Figure 14A); (3) neurons modulated by INT and either the nine spatial positions (INT+POS; Figure 14A) or (4) the epochs of interest (INT+EPO; Figure 14A). Comparing the results in the three areas, we have found no statistical differences between the four categories of task-related cells in both V6A and PEc, whereas some dissimilarities appeared between the two visuomotor areas and PE: compared with PE, V6A and PEc contain a higher percentage of neurons modulated by eye position, arm position or both (POS+EPO, V6A 52%, PEc 48%, PE 28%; see Figure 14A) and a higher incidence of neurons modulated by the interaction factor and target positions (INT+POS, V6A 16%, PEc 14%, PE 4%; see Figure 14A; z-test, V6A vs PE, POS+EPO p=1 x 10^{-7}, INT+POS, p = 0.0001; PEc vs PE, POS+EPO p=10^{-5}, INT+POS, p = 0.0009; V6A vs PEc POS+EPO p = 0.3, INT+POS, p = 0.5). Also, the proportion of cells modulated by the interaction factor and epochs (INT+EPO) was similar in V6A and PEc (z-test, V6A vs PEc p = 0.1) with a lower incidence of these cells in V6A compared with PE (z-test, V6A vs PE, p = 0.01) and no significant difference between PEc and PE (z-test, PEc vs PE p = 0.2; V6A 4%, PEc 7%, PE 10%; see Figure 14A). Cells modulated only by the interaction were similarly represented in all the three areas (V6A 3%, PEc 3%, PE 3%; see Fig. 11A; z-test, p > 0.05 for all comparisons).

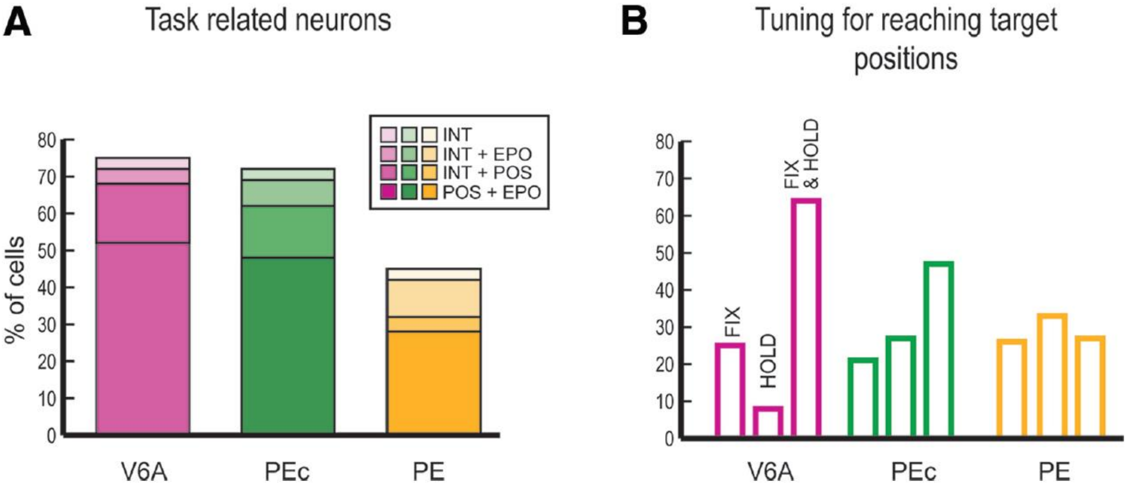

***Figure 14. Significant effects modulating V6A, PEc, and PE cells. A**, The histograms show the results of a two-way ANOVA as the incidence of cells modulated by the fixation and arm holding in space (EPO: epoch) and the nine spatial positions in one or both the epochs of interest (POS: target positions), or by the interaction of the two factors (INT: target positions*epoch). Numbers of modulated cells for each subgroup of task-related cells: POS+EPO, V6A N= 157, PEc = 126, PE = 52; INT+EPO, V6A N= 12, PEc = 18, PE = 19; INT+POS, V6A N= 47, PEc = 36, PE = 8; INT, V6A N= 10, PEc = 8, PE = 6 (cells with no effect, V6A N= 27, PEc = 22, PE = 36 not shown in figure). **B**, Percentages of cells tuned by the position of the reaching target in FIX, HOLD, and FIX&HOLD, as a result of a one-way ANOVA.*

6.2 A reverse trend of eye-hand position tuning in V6A/PEc and PE

To quantify the proportion of cells tuned by the target positions in FIX, HOLD, and in both epochs, we performed a one-way ANOVA ($p < 0.05$). Figure 14B shows the incidence of task-related cells tuned by eye positions (FIX) and/or arm positions in space (HOLD) separately for each area. We found that the distribution of V6A, PEc, and PE cells based on their tuning for reaching targets was different across task epochs (Figure 14B). Cells modulated only during FIX represented almost 30% of the total cell population in all three areas (z-test, $p > 0.05$ for all comparisons). Instead, cells modulated in HOLD and in both FIX and HOLD showed a clear and opposite trend from V6A to PE: cells modulated only by the position of the arm (HOLD) increased going from V6A to PE (z-test, V6A vs PEc, $p=4 \times 10^{-7}$; V6A vs PE, $p=7 \times 10^{-8}$), whereas cells modulated by eye-position and arm-position (FIX&HOLD) progressively decreased from V6A to PE (z-test, V6A vs PEc, $p = 0.0008$; V6A vs PE, $p=8 \times 10^{-9}$; PEc vs PE, $p = 0.002$). Moreover, within the same area we found some dissimilarities in the categories of cells spatially tuned in V6A and PEc, but not in PE. In V6A and PEc, cells spatially modulated during both FIX and HOLD were more represented (64% and 47% respectively) than those cells tuned only in one epoch (z-test, $p < 0.01$ for all comparisons), supporting the view that these areas are more implicated in eye-hand coordination, being highly sensitive to both the direction of gaze and to the arm proprioceptive signals. Furthermore, in V6A we observed a lower incidence of neurons modulated only during HOLD with respect to those modulated only during FIX (z-test, $p=3 \times 10^{-6}$), and this is in line with the increase of somatosensory and the simultaneous decrease of visual processing observed along the caudo-rostral axis of the medial SPL. In PE we did not find any statistical differences in the subgroups of cells (z-test, $p > 0.05$ for all comparisons).

To sum up, these results show the existence of a decreasing trend for cells spatially modulated during both fixation and arm holding going from V6A to PEc and then to PE. This coding scheme parallels the gradual shift from joint to separate processing of amplitude and directions signals of arm movement during reaching (Hadjidimitrakis et al., 2014a, 2015; De Vitis et al., 2019).

6.3 Dynamic space representation along the task

To characterize the spatial preference of task-related neurons during the time course of the task, a sliding window linear regression analysis was performed, considering target depth and direction as independent variables.

Neurons with a significant linear vergence tuning were classified as NEAR or FAR, whereas cells linearly tuned by version angle were classified as CONTRA or IPSI, depending on both the sign of the correlation coefficient and the recording hemisphere. The percentage of V6A, PEc, and PE cells falling into the above groups is illustrated in Figure 15. Regarding the neuronal preference for depth, V6A neurons equally represented NEAR and FAR reachable space during the time course of the task, with a slight preference for farther positions at the end of the holding phase (Figure 15, left, two-sample Kolmogorov Smirnov test, $p < 0.01$). PEc cells showed instead a stronger tuning for FAR space from the beginning of the trial (FIX, two-sample Kolmogorov–Smirnov test, $p < 0.01$), and this predominance was maintained until movement execution, after which, in the HOLD phase, the proportion of neurons preferring FAR positions matched that of neurons preferring NEAR positions (Figure 15, left, two-sample Kolmogorov–Smirnov test, $p > 0.05$). PE neurons tuned for FAR reachable space were found to be more represented than those tuned for NEAR space during the whole trial (Figure 15, left, two-sample Kolmogorov–Smirnov test, $p < 0.01$ in FIX and HOLD). This remarkable preference for FAR space likely reflects the strong influence of somatosensory input in PE. When the monkey reaches the farthest positions, the arm hyperextends to touch the target, and this leads to a strong somatosensory stimulation evoked by shoulder, elbow, and wrist rotation. Regarding the directional tuning (Figure 15, right), IPSI neurons were more numerous than CONTRA ones in V6A, particularly during target fixation and holding (two-sample Kolmogorov–Smirnov test, $p < 0.01$), whereas these two categories of neurons were equally represented in PEc (two-sample Kolmogorov–Smirnov test, $p > 0.05$ in FIX and HOLD). In turn, PE cells showed a gradual shift from a slight preference for the CONTRA space in the early part of the trial (two-sample Kolmogorov–Smirnov test, $p < 0.05$ in FIX) to a more pronounced preference for the IPSI space in HOLD (Figure 15, right, two-sample Kolmogorov–Smirnov test, $p < 0.01$).

We then investigated how constant the preference for a given position (i.e., NEAR vs FAR or IPSI vs CONTRA) during the time course of the task was. To evaluate the consistency of spatial preference across single neurons, we quantified the cells that retained, altered, lost, or acquired their spatial preference in couples of subsequent bins of 50 ms. The overall tendency of cells from all the three areas was to retain their spatial preference both in depth and direction (i.e., vergence and version). Cells that did not alter their preference as the task progressed were the most represented in all the three areas (50–60% in V6A, 40–50% in PEc, 30–40% in PE), from fixation onset until target pressing, both in depth and direction. The proportion of cells preserving their depth tuning slightly decreased during target holding (epoch HOLD) in all three areas (40% in V6A, 30–40% in PEc, 20–30% in PE). Only a minority of cells from all the three areas (10–15%) lost or acquired their tuning, and very few cells (< 3%) changed their spatial preference during the time course of the trial, both in depth and in direction. In summary, the trends were similar for all the three areas both in depth and direction, with a remarkably stable proportion of spatially tuned cells that retained their tuning as the trial progressed, from target fixation to LED pressing.

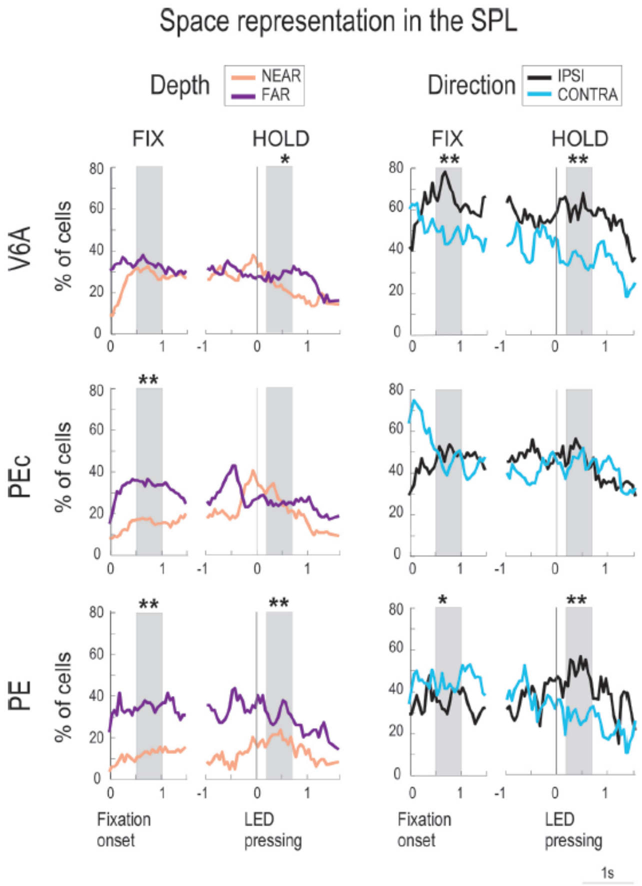

Figure 15. Space representation in the three SPL areas along the task. *Percentage of V6A (top), PEc (middle), and PE (bottom) task-related cells linearly modulated by depth (left) and direction (right) showing a preference for far (FAR, purple line) or near (NEAR, pink line) space and ipsilateral (IPSI, black line) or contralateral (CONTRA, light blue line) space with respect to the recording hemisphere in a sliding window linear regression (window-bin width: 250 ms; step: 50 ms). Asterisks indicate significant differences between curves in bins of 250ms (two-sample Kolmogorov–Smirnov test, p,0.01). Other conventions as in Figure 11.*

6.4 Population responses

The timing of neural activity during the task and the spatial tuning of cells modulated by eye-position and/or arm-position is evident from the population SDFs (see Materials and Methods) shown in Figure 16, where neural activity was ranked according to each cell's preference in FIX (Figure 16A) and HOLD (Figure 16B). In Figure 16A-B, cell responses were classified from the strongest one, elicited by a certain target position for a given neuron (whatever the position of the target was), hereafter called BEST, the second-best response, the third, the fourth, and so on, up to the ninth, corresponding to the weakest response for the same neuron, hereafter called WORST, during FIX and HOLD epochs, respectively. After ranking the neural activities according to the spatial preferences during FIX, we found that the activity during fixation started to diverge around the fixation onset in V6A and PEc (Figure 16A, top and middle panels, permutation test, best vs worst curves, V6A p = 0.003, PEc p = 0.008), while in PE neural responses diverged later, after the fixation onset (Figure 16A, bottom panels, permutation test, PE p = 0.004). The size of the tuning was similar in the three areas in FIX, but the modulation lasted longer in V6A and PEc than in PE (compare the significance bars reported in each panel). After ranking the neural activities according to spatial preferences during HOLD, we still found a tuning effect during FIX in V6A (Figure 16B, top panels), where BEST and WORST position lines started to diverge 40ms after the fixation onset and remained well separated for the remaining part of the trial (permutation test, best vs worst curves, V6A $p = 0.007$). During HOLD, the activity in V6A was strongly tuned: the curves for all nine conditions appeared to be unraveled and well distinct, with activities for the BEST and second-best conditions being continuously higher than the baseline (FIX activity), and the ones for conditions seventh, eighth, and WORST being progressively more inhibited than the activity during FIX. In PEc (Figure 16B, middle panels), the modulation during FIX, although significant (permutation test, best vs worst curves, PEc $p= 0.008$), was much weaker than in V6A, and in PE (Figure 16B, bottom panels) it was completely absent ($p > 0.05$). During HOLD, the same strong tuning was present in PEc and PE, and it looked similar in the three areas. It is also evident, though not indicated by a specific epoch in Figure 16, that the activity during the execution of arm movement (the period just before the alignment to the LED pressing) was strongly tuned in V6A and PEc and weaker in PE. Interestingly, while in V6A and, although to a lesser extent, PEc, the spatial tuning was evident during both FIX and HOLD, regardless of the epoch on which the ranking was based (Figure 16A and 16B), in PE the modulations were evident only if the ranking was made according to the given epoch (i.e., clear tuning in FIX and no modulation in HOLD if the ranking was based on the activity in FIX, Figure 16A; the opposite trend if the ranking was based on the activity in HOLD, Figure 16B). This suggests that the ranking orders in PE were different during fixation and arm holding, and that the neural representations of these two signals (eye position, proprioception) in PE are independent.

To sum up, V6A and PEc neurons showed similar temporal evolution in both FIX and HOLD, being their activity jointly influenced by eye position and arm movement-related information, whereas PE cells seemed to be more involved in the encoding of proprioceptive signals from the arm rather than oculomotor signals.

As evident from the population data, the activity for the WORST position in HOLD is lower than in FIX. This suggests that cells could be further inhibited by the position of the arm, in addition to the inhibition because of eye position. So, we calculated the incidence of task-related cells excited (i.e., with a higher firing rate) or inhibited (i.e., with a lower firing rate) during HOLD with respect to the baseline activity (FIX) in each target position. As expected, we found more cells inhibited than cells excited in all the three SPL areas we tested: 33 cells inhibited (15%) and 9 excited (4%) in V6A (z-test, V6A $p = 0.0001$), 25 cells inhibited (13%) and 10 excited (5%) in PEc (z-test, PEc $p = 0.01$) and 12 cells inhibited (14%) and 4 excited (5%) in PE (z-test, PE $p = 0.04$). The incidence of inhibition was similar among the three areas.

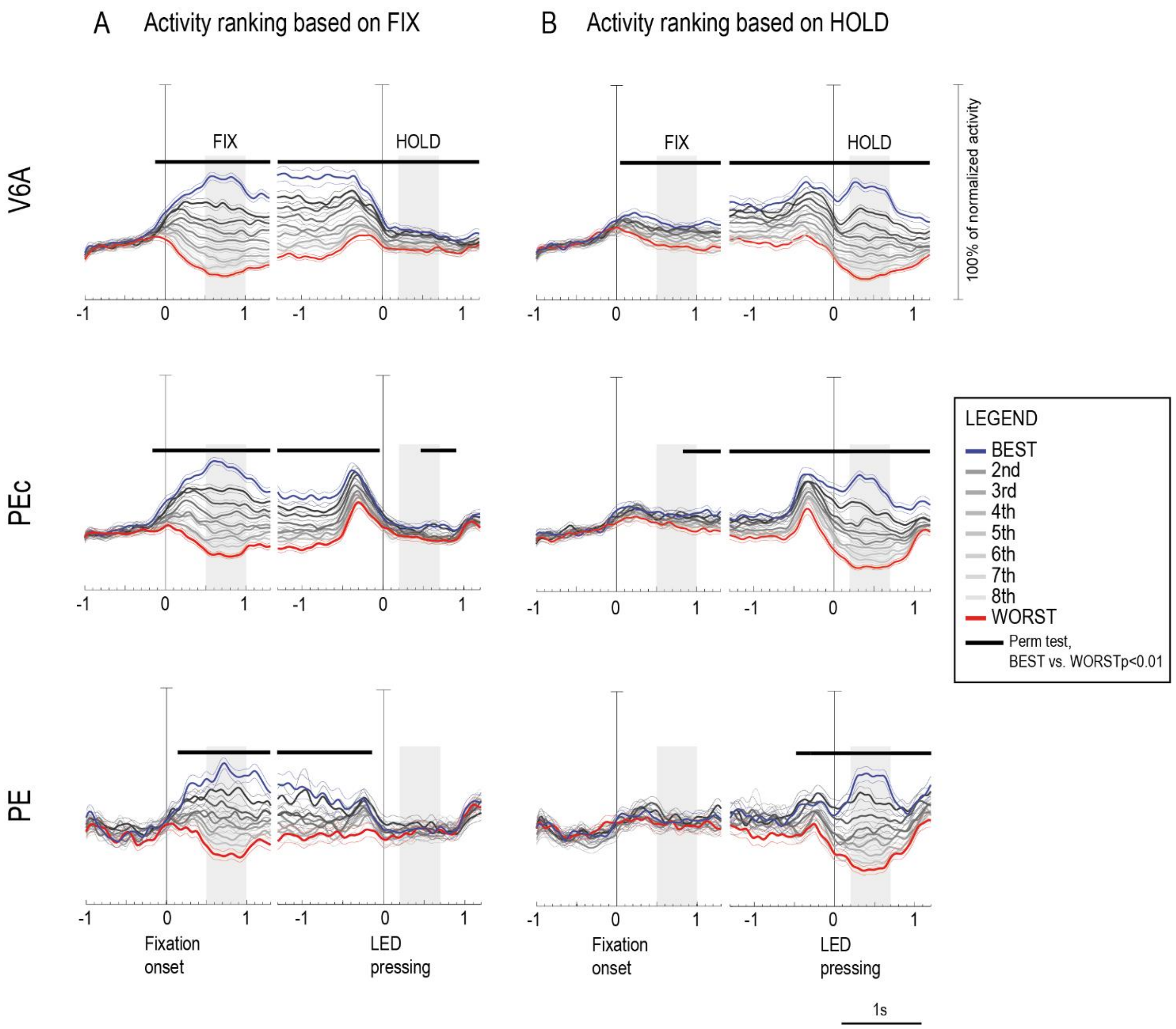

***Figure 16. Population activity**. Population activity of V6A (top), PEc (middle), and PE (bottom) cells modulated by the position of reaching target during FIX and/or HOLD, expressed as averaged normalized SDFs (thick lines) with variability bands (SEM; thin lines). **A**, SDFs obtained by ranking the activity of each neuron according to the intensity of the response for each spatial position elicited in FIX for that neuron. **B**, SDFs obtained ranking the activity of each neuron according to the intensity of the response for each spatial position elicited in HOLD. Neuronal activities have been aligned twice at the onset of fixation and at LED pressing. Vertical bars in all SDF plots: 100% of normalized activity. Permutation test was performed on BEST (blue line) and WORST (red line) curves in all the time intervals shown. At the top of each panel, black bars are used to indicate the significancy (see legend)*

7. DISCUSSION

In this thesis we examined the effect of eye- and arm-position signals on neuronal activity in SPL areas V6A, PEc and PE while two monkeys were required to fixate and maintain the hand on foveated reaching targets, located in the 3D space. Present data point out that in V6A and PEc a similar processing of these stimuli, different than PE, occurs. This finding supports the recent view that PEc is not part with PE to BA5 but instead it belongs to BA7 as V6A, having more structural and functional features in common with this area, in comparison to PE (Gamberini et al., 2020).

We found a major incidence of task-related cells in V6A and PEc than in PE (75% in V6A; 71% in PEc; 45% in PE) and V6A and PEc neurons exhibited similar spatial patterns of neural modulation during fixation and target holding, according to the target position. In contrast, in PE the neural representations during fixation and target holding were not joined, suggesting an independent encoding of eye and arm position. A similar trend has been observed in the neural processing of amplitude and direction of arm movement during reaching: in PE the neural substrates related to amplitude and direction were different (Lacquaniti et al., 1995; De Vitis et al., 2019), while in V6A and PEc a common neural substrate was observed (Hadjidimitrakis et al., 2014a, 2015). In the study of Lacquaniti, the activity of PE neurons was recorded when the animal was required to perform movements of constant amplitude from one of three possible starting points to one of eight possible directions. The neurons were classified on the basis of the relative contribution of azimuth, elevation, and distance and it was found that most of them (about 70%) clustered around the cardinal spatial axes for the activity during both stationary posture at the target (Figure 17A) and the execution of reaching movement (Figure 17B). Moreover, neurons modulated by target distance were twice as much as those modulated by azimuth and elevation.

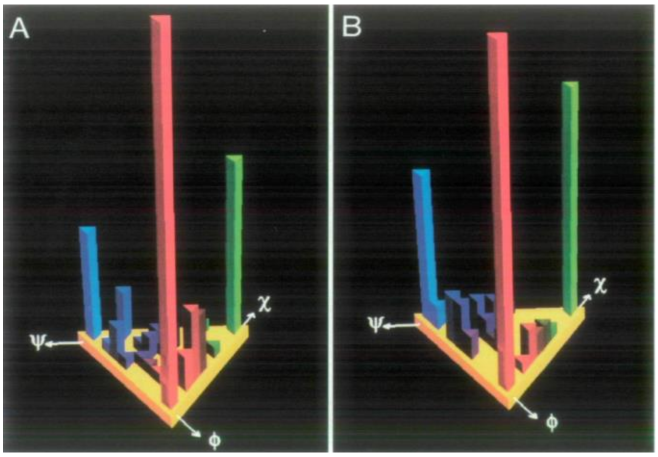

Figure 17. Histograms of the distribution of all neurons over the base of homogeneous coordinates*. The coordinates have been discretized in 0.1-unit intervals. The height of the prisms is proportional to the number of cells whose coordinates fall in a given interval. Prisms at the azimuthal vertex (coordinates 1, 0, 0) are in green, at the elevation vertex (0,1, 0) in blue, and at the distance vertex (0, 0,1) in red. Prisms at intermediate locations are color coded in proportion to the distance from each vertex.* ***A****, THT activity;* ***B****, MT activity (from Lacquaniti et al., 1995).*

Similar findings were reported in the medial sector of PE through the same task paradigm used in this study with nine fixation and reaching targets located in the 3D space. De Vitis and colleagues reported that the most represented classes of tuned cells in area PE were related to neurons modulated only by depth or only by direction. During the behavioural task the incidence of cells modulated by depth significantly increased from the fixation time when the animal was required to maintain the gaze on the cued target (EARLY FIX and LATE FIX, Figure 18A) to the arm movement and holding target time (REACH and HOLD, Figure 18A). On the contrary, the direction tuning was high in the first part of the fixation time (EARLY FIX) then tended to decrease with a slight increase during HOLD. A low proportion of cells was modulated by both signals across epochs in agreement with the suggested idea that in PE occurs a separated encoding of depth and direction signals. Figure 18B remarks the temporal evolution of spatial tuning in PE using a sliding window analysis (width: 200 ms, step: 50 ms) confirming a great distinction between the percentage of cells modulated by depth and directions specifically after movement onset.

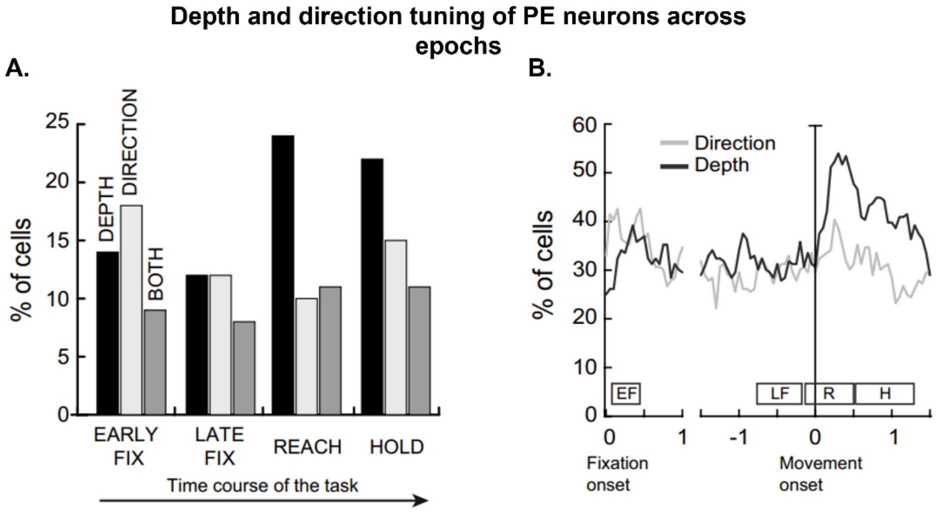

***Figure 18. Distribution of the incidence of significant effects modulating PE cells and strength of depth and directional tuning. A**, Histogram shows the results of a two-way ANOVA (factors: DEPTH and DIRECTION, $p < 0.05$) as incidence of modulated cells during the target fixation (epoch EARLY FIX), reaching preparation (epoch LATE FIX), execution (epoch REACH) and LED pressing (epoch HOLD). **B**, Percentage of tuned cells by depth (black line) and direction (gray line) in a sliding window ANOVA (width: 200 ms, step: 50 ms). Trials are aligned to fixation and movement onsets. Rectangles below each plot indicate the functional time epochs ('EF', EARLY FIX; 'LF', LATE FIX; 'R', REACH; 'H', HOLD) (modified from De Vitis et al., 2019).*

In previous works performed by Hadjidimitrakis and colleagues, the activity of V6A and PEc neurons was tested in the same experimental conditions. Differently than PE, it was found that in V6A and PEc are more represented cells that encode depth and direction signals jointly during all the phases of the task. Figure 19A shows the spatial tuning in area V6A. During target fixation (FIX), a similar number of cells were modulated by depth only, direction only, and both signals. As the task progressed, the percentage of neurons modulated by direction only significantly decreased whereas cells jointly sensitive to both the parameters, which were well represented in all epochs, slightly increased. Figure 19B reports an example of V6A neuron modulated by both the parameters, tuned by depth in all epochs with a preference for intermediate to far positions and by direction during both fixation and arm movement planning, showing higher activity for contralateral positions.

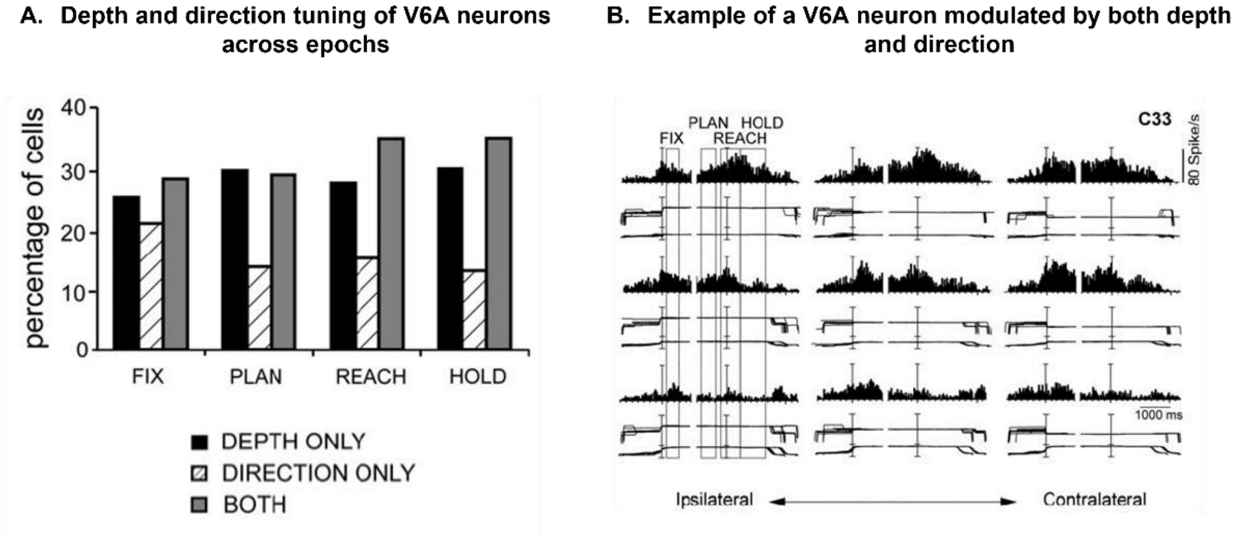

Figure 19. Incidence of depth and direction tuning during each task epoch in V6A and example of a V6A neuron modulated by the two parameters. A*, Percentage of neurons with tuning for depth only (black), direction only (white), or both signals (gray) during several task epochs (fixation, planning, movement, and holding, ANOVA, P<0.05).* ***B****, Depth and direction tuning in several epochs of the task in an example V6A neuron. Spike histograms and version and vergence eye traces are shown for the 9 target positions. Rows represent the 3 depths (far, intermediate, near) and columns the 3 directions (contralateral, center, ipsilateral). Vertical lines indicate the alignment of activity and eye position traces at the onset of fixation and at the onset of arm movement. Realignment is evidenced with a gap in histograms and eye traces (modified from Hadjidimitrakis et al., 2014a).*

Figure 20A reports the spatial tuning during the task epochs in PEc. The proportion of neurons that showed only depth modulations consistently increased as the task progressed from Fix to Reach epoch. In contrast, the percentage of cells showing only an effect of direction was highest in FIX and decreased to constant levels in the following intervals of time. As in V6A, the incidence of cells modulated by both signals increased gradually being significantly higher during arm movement and target holding with respect to the beginning of fixation. Figure 20B illustrates an example of a PEc neuron tuned by both depth and direction. This neuron was strongly activated only when the monkey performed the task for the far, contralateral target, with the cell's firing being much weaker or absent for the other target locations.

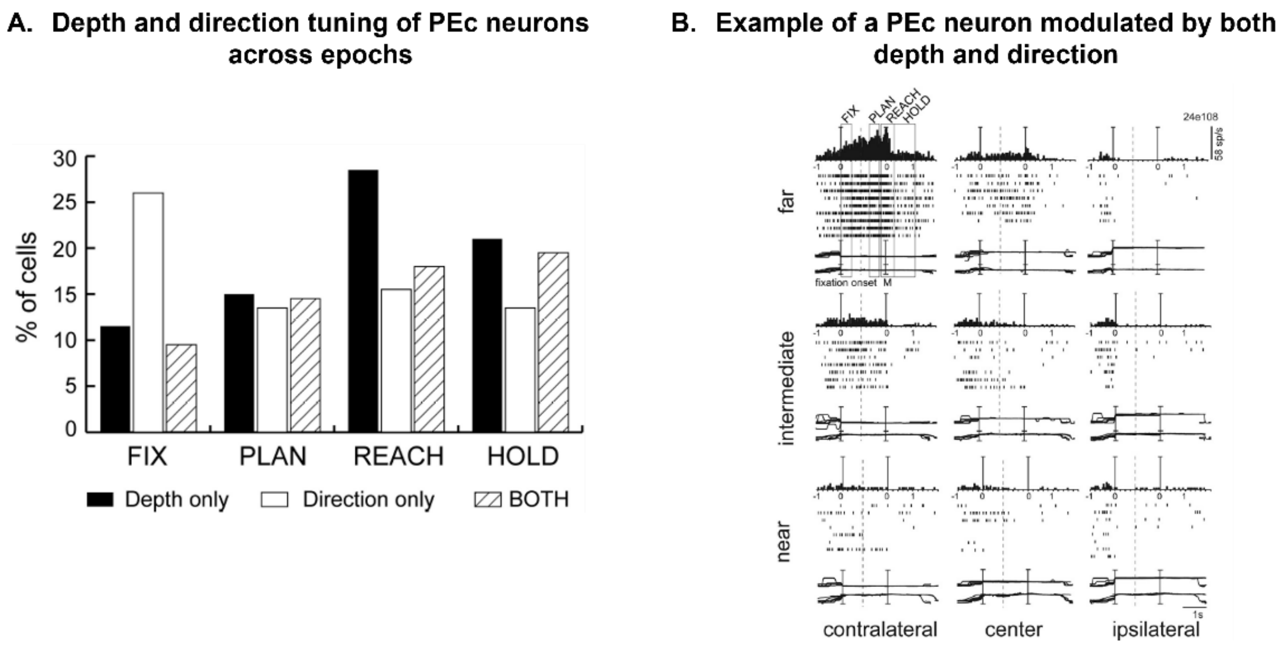

A. Depth and direction tuning of PEc neurons across epochs

B. Example of a PEc neuron modulated by both depth and direction

Figure 20. Incidence of depth and direction tuning during each task epoch in PEc and example of a PEc neuron modulated by the two parameters. A*, Percentage of cells in the population of PEc with tuning for depth only (solid), direction only (open), and both signals (hatched) during different task epochs (Fix, Plan, Reach, and Hold).* **B***, Depth and direction tuning in several epochs of the task in an example PEc neuron. Spike histograms (top), rasters (middle), and version (upper) and vergence (lower) eye position traces (bottom) are shown for the 9 target positions. Realignment is evidenced with a vertical dashed line. All other conventions as in Figure 19 (modified from Hadjidimitrakis et al., 2015).*

The idea suggested by Hadjidimitrakis and colleagues (2014a) about this discrepancy in the encoding of the two parameters in the PPC is that areas receiving predominantly visual input, such as V6A and PEc, tend to process jointly target distance and direction information, whereas those that receive mainly somatosensory input are more likely to represent spatial parameters separately (Figure 21).

In V6A and PEc visual and eye positions information are implemented to build a 3D map of the spatial locations that can be reached out by hands. Noteworthy, eye positions signals activate V6A specifically when targets are located in the peripersonal rather than in extrapersonal space, which is out of the reachable environment (Hadjidimitrakis et al. 2011) and when saccades brought the eye to a spatial location that is also target for hand movement (Battaglia-Mayer et al. 2000).

Area PE, on the contrary, does not receive visual information (Johnson et al. 1996), and vergence angle influences the reaching activity of a small fraction of PE cells (Ferraina et al. 2009). Moreover, S1 which is likely to send somatosensory input to PE, also contains cells more sensitive to movement amplitude than to direction (Tillery et al. 1996) indicating that these somatosensory areas are more involved in the fine processing of spatial parameters.

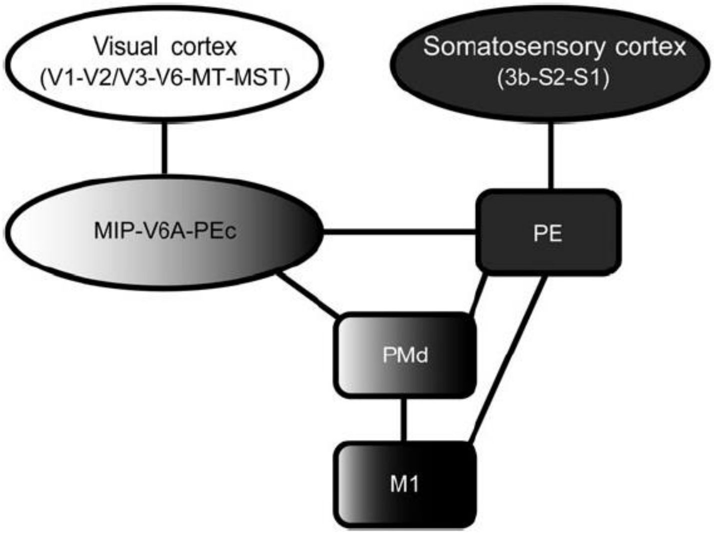

Figure 21. Distance and direction coding in the cortical reach-related areas. *Areas are depicted in different grayscale gradients according to the relative proportion of visual (white) and proprioceptive (black) information they receive. V1: primary visual cortex; V2: area V2; V3: area V3; V6: area V6; MT: middle temporal area; MST: medial superior temporal area; S1: primary somatosensory cortex; S2: secondary somatosensory area; 3b: area 3b ; MIP: area MIP; V6A: area V6A; PEc: area PEc; PE: area PE; PMd: dorsal premotor area PMd; M1: primary motor area (modified from Hadjidimitrakis et al., 2014a).*

Our data showed that the modulating effect of eye and arm-positions followed two functional trends: a decreasing one for cells spatially tuned during both fixation and arm holding going from V6A to PEc, and then to PE, and an increasing one related to the incidence of cells modulated only during arm holding, which was much lower in V6A compared to PEc and PE (see Figure 14B).

This result are consistent with the well accepted idea of a functional gradient in the SPL proceeding in caudo-rostral direction which consists in a decrease of visual and concomitant increase of somatosensory processing.

As mentioned before (see Introduction) V6A receives predominantly visual and eye position input with a high percentage of neurons (74%) modulated by the direction of gaze and/or the fixation in depth (Breveglieri et al. 2012). A lower fraction of V6A cells is sensitive to somatosensory inputs coming from both proximal and distal parts of upper limbs (about 30%; Breveglieri et al. 2002). On the contrary, in PEc neurons sensitive to somatosensory signals are more common than cells with visual properties (about 65%; Breveglieri et al., 2006, 2008; Gamberini et al., 2018) and the incidence of somatosensory neurons increases going to PE (more than 90%; Sakata et al., 1973; Mountcastle et al., 1975; De Vitis et al., 2019). In line with this trend, it has been reported a higher presence of eye-centered and mixed (eye/hand-centered) cells in V6A (Bosco et al., 2016) and stronger employment of hand-centered reference frame in PEc (Hadjidimitrakis, et al., 2014b; Piserchia et al., 2017) and PE (Lacquaniti et al., 1995).

The reported major incidence of cells with a mix of gaze and arm signals in V6A and PEc (see Figure 14B) is also supported by the study of Battaglia-Mayer and colleagues (2001) where several behavioural tasks assessed in both areas that retinal-,eye- and hand-related signals converge in the activity of most cells.
Moreover, it has been documented that both V6A and PEc are bimodal areas; they host bimodal neurons able to process signals belonging to both sensory modalities (Breveglieri et al. 2008, Gamberini et al. 2018).
Another recent study revealed that the majority of cells in V6A are not selective only for one factor but are characterized by "mixed selectivity" which is the ability of a neuron to respond to several kinds of signals (Diomedi et al 2020). It has been demonstrated that in V6A it is possible to build a functional fingertip for each neuron, indicating the combination of parameters which better explain its activity. Authors investigated also the temporal evolution of the V6A population discharge during a fixation-to-reach task and found a different correlation of the neural activity between the first part of the trial and the planning, movement, and target holding phases. This change could reflect a shift from a visual code to a more motor-related one or, alternatively, the superimposition of motor-related and proprioceptive information with previous underlying visual-related inputs. This result highlights the occurrence in V6A of sequential visuospatial transformations which are important to guide arm movement.
Therefore, the confirmed mixed encoding of V6A and PEc, higher with respect to PE, supports the view that these areas are more implicated in the eye-hand coordination during goal directed actions.

7.1 Role of PE in encoding arm posture

While in the motor cortex the maintenance of a steady position of the arm is more related to the patterns of muscular contraction rather than to the posture per se (Evarts, 1969; Cheney and Fetz, 1980; Fromm, 1983), the sensitivity of the majority of Brodmann's area 5 cells to passive movements of the limbs (Sakata et al., 1973; Mountcastle et al., 1975) and to static arm positions (Georgopoulos et al., 1984; Kalaska and Hyde, 1985; Hamel-Pâquet et al., 2006; Cui and Andersen, 2011; McGuire and Sabes, 2011; Shi et al., 2013; De Vitis et al., 2019) suggested a major role of this parietal area in encoding arm posture, in agreement with the current results regarding area PE. Despite the impact of the above cited papers about PE functional properties, only a few studies addressed the relative contribution of gaze direction and static hand positions signals in PE (Ferraina et al., 2009; De Vitis et al., 2019). Ferraina's results highlighted the effect of both eye and hand information on PE neuronal activity, with a prevalence of hand information. Conversely, our results suggest a similar encoding of eye and arm signals in PE. The discrepancy could be due to the different experimental conditions, being the task used by Ferraina and co-workers a non-foveated reaching task, where arm-target positions changed while the coordinates of fixation-target remained constant. Another explanation could be the difference in the recording sites, since they studied a lateral sector of area PE, that only partially overlapped with our recording region (De Vitis et al., 2019).

Moreover, the data shown in Figures 14B and 16 suggest that an independent encoding of ocular and hand signals occurs in PE. As discussed in the previous paragraph, as PE is prevalently a somatosensory area, it is likely to perform a more specialized analysis of sensory signals than regions located more caudally in the SPL, like PEc and V6A which receive and elaborate also visual input.

Furthermore, we have found that a large proportion of PE cells tuned by depth showed a bias for FAR reachable space (Figure 15), which most likely reflects a movement amplitude, corroborating the view that PE is involved in processing somatosensory and proprioceptive signals from the arm. Postural adjustments could be more important when the monkey reaches and holds the farthest targets and the integration of somatosensory and proprioceptive inputs from the arm could be reflected in increased levels of neural activity.

7.2 Possible influence of spatial attention shifts on V6A activity

Given the foveal nature of the reaching movements in our task, we cannot exclude that the responses observed during static arm positions could also reflect the spatial attention directed to the target besides the gaze (eye position) and the proprioceptive cues (arm position). In fact, it was demonstrated that shifts of covert attention modulate the activity of V6A cells (Galletti et al 2010), a result confirmed by fMRI (Caspari et al 2015). Several monkey and human experiments have revealed a crucial role of SPL during both overt and covert spatial attention shifts (Vandenberghe et al., 2001; Yantis et al., 2002; Molenberghs et al., 2007; Kelley et al., 2008; Galletti et al., 2010; Ciavarro et al., 2013; Caspari et al., 2015, 2018; Arsenault et al., 2018). In 2010, Galletti et al. showed for the first time attention-related activity in V6A at neural single cell level using a task where the monkey was required to covertly shift its attention from a central fixation point towards a peripheral location, and vice versa (Figure 22A).

They found that the neural modulation was still present when attention was covertly shifted outward, to a peripheral cue, and demonstrated that visual, motor, and attentional responses can occur in combination in single V6A neurons (example of a V6A neuron modulated by covert shift of attention in low space is shown in Figure 22B) (Galletti et al 2010).

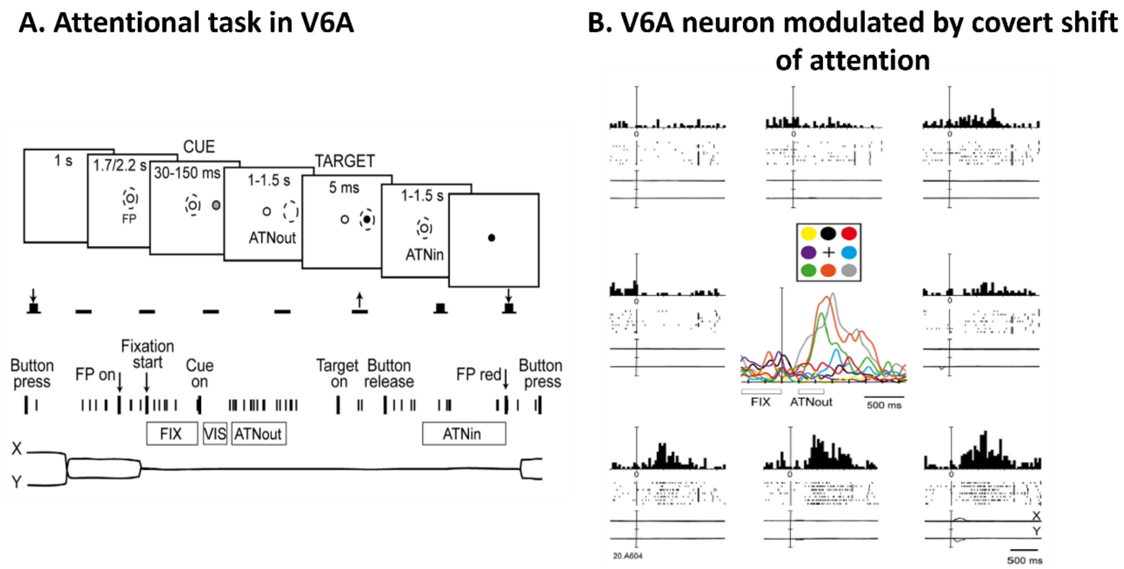

Figure 22. Attentional task and effect of covert shift of attention in V6A example neuron*. *A*,** *Schematic representation of the task. Top: Sequence of events in a single trial. After button pressing, the monkey maintained fixation on the central fixation point (white dot, FP) all throughout the trial while covertly shifting attention (dashed circle) towards the cued location (grey dot). After target (black dot) detection, the animal released the button, continuing to gaze the fixation point until it changed in color (from green to red). Color-change detection was reported by the animal by button pressing. Bottom: typical example of neural activity and eye traces during a single trial. Short vertical ticks are spikes. Long vertical ticks among spikes indicate the occurrence of behavioral events (markers). Below the neural trace, time epochs during a typical trial are indicated. FIX: fixation epoch, VIS: visual epoch, ATNout: outward attention epoch, ATNin: inward attention epoch.* ***B, *Example of spatially-tuned modulations of neural activity during outward attention epoch. The neuron shows a strong discharge during outward attention epoch preferring covert shifts of attention towards the bottom part of the space. Each inset contains the perievent time histogram, raster plots and eye position signals, and is positioned in the same relative position as the cue on the panel. In the central part of the figure, the spike density functions (SDFs) of the activity for each of the 8 cue positions are superimposed and aligned on the cue onset. Neural activity and eye traces are aligned on the cue onset. Scalebar in peri-event time histograms, 70 spikes/s (modified from Galletti et al. 2010).*

More recently, Caspari and collaborators (2015) identified a network of areas in monkeys, including parietal area V6A, activated during spatial shifting events, using a spatial attention task adapted from a human fMRI study (Molenberghs et al., 2007).

These findings could explain the proportion of V6A cells that we found to be inhibited during HOLD, possibly due to the modulating effect of the spotlight of attention. During HOLD, the spatial attention is likely to be covertly shifted out of the reaching target because the animal at that time has a more attractive object to attend, the home button, that must be reached by its hand soon after the HOLD period to receive a reward. This keeps well with the results of Galletti and colleagues (2010) that reported excitations or inhibitions of the neural activity with inhibited cells more sensitive to the direction of covert attention than excited cells, showing higher number of cells with high direction selectivity (Figure 23A-B).

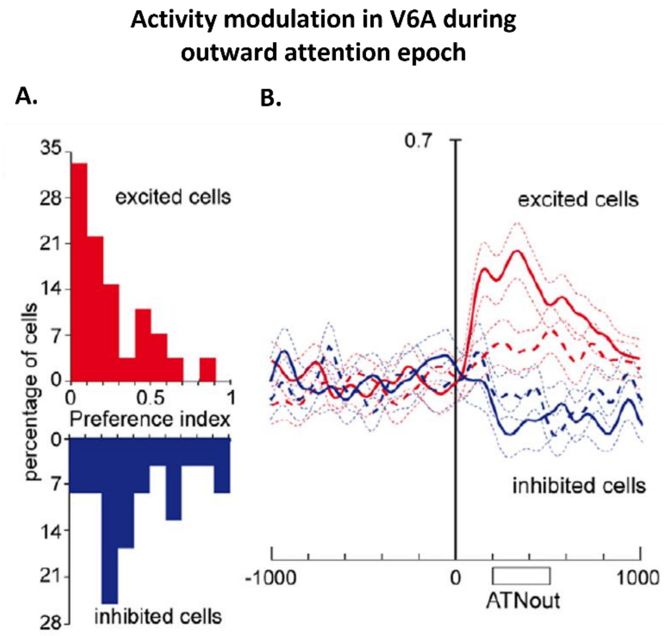

***Figure 23. Activity modulation in V6A during outward attention epoch**. **A**, Distribution of preference index (PI) for excited (red histogram) and inhibited (blue histogram) cells. Preference index indicate the direction selectivity of neurons modulated during outward attention epoch computed as: PI = abs(D-OD)/(D+OD), where D= maximal discharge for cells excited with respect to the fixation time (FIX) or minimal discharge for cells inhibited with respect to FIX, and OD = discharge for the opposite position. PI ranged from 0 to 1. **B**, Effect of the covert dislocation of the spotlight of attention on the activity of V6A cells during outward attention epoch. The average SDF for the excited (red lines) and inhibited (blue lines) cells are shown. Continuous lines represent the average SDF for the cue location evoking the maximal (excited cells) or minimal (inhibited cells) activity, and the dashed line that for the opposite location. Two dotted lines for each SDF indicate the variability band (SEM). The activity of cells in each population is aligned on the cue onset. Scale in abscissa: 200 ms/division; vertical scale 0.7 (Galletti et al. 2010).*

We observed a similar percentage of cells inhibited during the target holding in all the SPL areas considered here (15% in V6A, 13% in PEc, 14% in PE), and inhibited cells were also found by Gardner et al. (2007) in PE (41%) and AIP (38%) during the holding period after a grasping movement in a reach-to-grasp task. The inhibition was particularly relevant near the end of the holding period, just before the start of the backward arm movement to reach the initial hand position. Even in this case, the spatial attention shifts (from positions on the panel, the reaching targets, to a position near the trunk, the home button) could explain the observed results.

7.3 Human homologues of PE, PEc, and V6A

Recently, structural and functional studies have revealed the existence of the putative human counterparts of macaque monkeys' areas here studied. In humans, BA5 is subdivided in two mesial areas, 5Ci (cingulate parietal) and 5M (medial parietal), and one lateral area (5L) located in the rostral bank of the post-central sulcus.

The distribution of the receptors of the main neurotransmitter families suggest that 5L and 5M are likely to be equivalent of macaque's area PE (Scheperjans et al., 2005a; Scheperjans et al., 2005b)

In macaque, BA5 extends in the lateral part of the brain whereas in human it is confined in a more medial region. Gamberini and colleagues (2020) propose that this difference is caused by the expansion of the inferior parietal cortex during evolution which could have 'pushed' upward and medially BA5, therefore despite the location the functional characteristic are equivalent.

For example, based on collected fMRI data, Sereno and colleagues found the presence of a second somatosensory homunculus (Parietal Body Area, PBA) in human SPL posteriorly to the SI which resembles the rough topographical map of the body present in macaque area PE (for review Huang and Sereno 2018). Moreover, PBA is activated by goal-directed limb movements, but it is not organized topographically similarly to what has been observed in macaque in the posteromedial part of PE (De Vitis et al. 2019) and in PEc (Gamberini et al. 2018).

In humans, BA7 has been split into area 7PC, located in the posterior wall of the post-central sulcus, 7A and 7P in the anterior and posterior part of dorsal SPL, respectively, and 7M in the medial wall (Scheperjans et al., 2005a; Scheperjans et al., 2005b). The macaque equivalent of these areas would be areas MIP and/or PEip, PEc, V6A and PGm respectively (Gamberini et al. 2020; Caminiti et al. 2015).

Supporting the idea of a strict homology between human and non-human primate SPLs, in a recent neuroimaging study, Pitzalis and colleagues (2019) reported the putative human homologue location of areas V6A, PEc and PE. The human area (h) V6A occupies the posterior portion of SPL, anterior to the POs, in a cortical region that includes the caudalmost portion of the precuneate cortex. Therefore, hV6A is on the exposed parietal cortex differently to its location in monkey brain where V6A is hidden in the anterior bank of POs. hV6A borders anteriorly with hV6 (Pitzalis et al. 2006) and posteriorly with hPEc, which occupies the dorsalmost portion of the anterior precuneus; area hPE is anterior to hPEc and occupies the dorsomedial portion of the post-central gyrus, just over the tip of the cingulate sulcus (Figure 24).

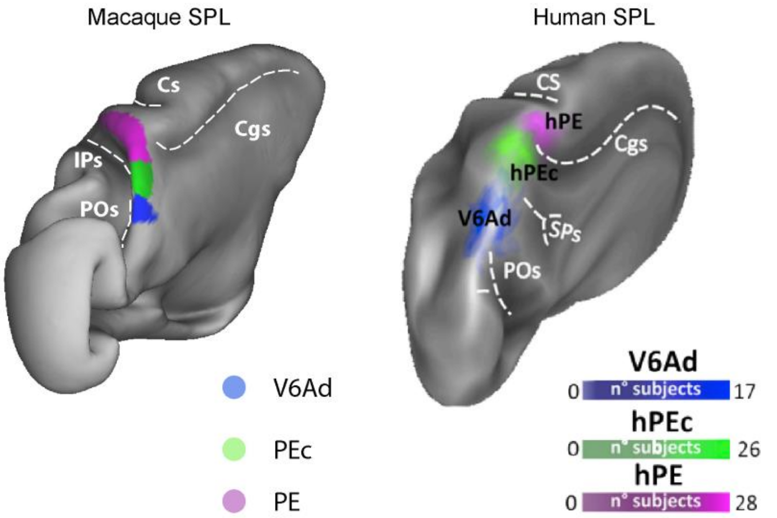

Figure 24. Homologies between some SPL areas in macaque and human brain. *3D reconstructions of the postero-medial view of a left hemisphere of the macaque (left) and of the human (right), not in scale.* ***Left****, Extent and location of the cytoarchitectonically defined areas V6A, PEc and PE. The borders were obtained overlapping retinotopic and functional properties of single neurons and cytoarchitectonic features in monkeys (Galletti et al. 1996, Gamberini et al. 2011, Gamberini et al. 2018).* ***Right****, Extent and location of hV6Ad, hPEc and hPE (Pitzalis et al. 2019, Fattori et al. 2005). Individual ROIs are overlapped into Conte69 brain atlas to form group probabilistic ROIs. The color scale indicates the proportion of subjects whose ROI included that surface node, thus the probability that the node is included in the ROI. Dotted line indicates the fundus of main sulci: Cgs, cingulate sulcus; CS, central sulcus; IPs, intraparietal sulcus; POs, parieto-occipital sulcus; SPs, sub-parietal sulcus (from Passarelli et al. 2021).*

Moreover, it has been demonstrated that lesions in human and in nonhuman SPL areas result in a deficit in the eye-hand coordination. Optic ataxia (OA) is an example of neurological disease associated to lesions in the dorsal visual stream. OA patients are not able to perform visually-guided reach and grasp actions properly (Perenin and Vighetto, 1988; Battaglini et al., 2002; Karnath and Perenin et al., 2005) . In the next paragraph, I will describe the impairments in the integration of eye and limb position information in OA patients.

7.4 SPL lesions impair visuomotor coordination during reaching

The SPL sectors studied here are often damaged in patients affected by optic ataxia (OA), a visuomotor coordination deficit that strongly impairs reaching actions (Rossetti et al., 2019). OA is often associated with Balint's syndrome, a neurophysiological disease first described by the Hungarian neurologist Rezso Balint in 1909 which includes also; ocular apraxia, consisting in the difficulty in shifting the gaze voluntarily to a visual target and simultanagnosia, which is the inability to perceive at once time the several items of a visual scene. Optic ataxia occurring in isolation without the other symptoms of Balint's syndrome, is a rarer condition since it is caused by more localized and discrete bilateral or unilateral lesions which affect the SPL and areas around the intraparietal sulcus.

Very recent studies on OA patients performing reaching actions relying exclusively on proprioception showed that SPL lesions cause larger position errors than in healthy controls (Bartolo et al., 2018; Mikula et al., 2021).

These studies highlight the crucial role of these regions in using proprioceptive information about hand position to correctly direct reaching movements (Mikula et al., 2021).

Present data on single cells recording from monkey SPL may be the neurophysiological counterpart of this finding, with a deeper understanding of the stronger role of PE in estimating hand position basing on proprioceptive information and of V6A and PEc in linking this input with gaze-related signals as well as visual inputs. Indeed, in the study of Mikula and colleague it was found that when a unilateral OA patient was required to maintain fixation on a reaching target the drift was greater when he executed the movement with the ipsilesional (healthy) hand compared to his contralesional (ataxic) hand (Mikula et al 2021). The explanation to this result is that the movement of the healthy hand was executed in the contralesional space, indicating that the damage in the PPC had led to an impairment of the perception of limb position in oculocentric coordinates. Similar result was found also in a previous study where unilateral OA patients showed larger reach errors when the reach target was in the visual field contralateral to the lesioned hemisphere (Khan et al., 2007). These findings are in agreement with studies that suggest that proprioceptive information is integrated in the PPC into a gaze-centered coordinate system (Buneo et al., 2002; Colby et al., 1995; Medendorp et al., 2003, 2005). These studies are in accordance with present data confirming that in the SPL the concurrent encoding of gaze and proprioceptive signals is necessary to correctly estimate the hand position in the space.

All these areas are well equipped to contribute to the state estimation about upper limb status for controlling the correct execution of reaching movements (Fattori et al., 2017).

7.5 Towards an integrated view about perception and movement

Albert and colleagues (2020) challenged the idea that posture and movement are controlled independently, in contrast with models assuming that commands that hold the limb at a target location do not depend on the commands that moved the limb to that location (Yadav and Sainburg, 2011; Lametti et al., 2007; Todorov and Jordan, 2002; Ghez et al., 2007). In particular, by measuring activity across arm muscles during arm reaching and fingers movement they found that the hold period activity was related to the preceding movement period activity (Albert et al 2020).

Results showed that change in the hold period activity of a given muscle from the holding time that precedes reach onset to the holding time when the hand is at the target location, was approximately proportional to the integral of its activity during the reach period. Therefore, they proposed a model in which the integral of motor commands is added to initial hold activity, yielding a feedforward estimate of the commands required for holding still. Considering that transient inhibition of the motor cortex during a reach results in ‘freezing of the arm’ at its current posture, and not loss of muscle tone (Guo et al., 2015), they suggest that a distinct structure possibly in a subcortical area integrates the cortically-generated reach commands until the moment of cortical inhibition, and thus maintains posture despite removal of reach commands. In summary, according to this model the postural controller possesses a feedforward module that uses move commands to calculate a component of hold commands. This computation may arise within an unknown subcortical system that integrates cortical commands to stabilize limb posture (Albert et al 2020).

The adjustments performed during movement result from the integration of sensory feedback that enable a continuous monitoring of the state of the body and the world.

The importance of sensory feedback is evidenced in the optimal feedback control (OFC) theory (Todorov, 2004). According to the OFC theory, in order to make a movement, our brain needs to accurately predict the sensory consequences of our motor commands, combine these predictions with actual sensory feedback to form a belief about the state of our body and the world (called state estimation) and adjust our state producing those motor command that maximize the performance of the desired action (called optimal control) (Figure 25A) (Shadmehr and Krakauer, 2008). Based on this theory, Medendorp and Heed (2019) claim that sensation and movement are merely inseparable aspects of an action control asserting also that integrating rather than contrasting views on the perceptual and motor function in PPC may better explain its overarching functional organization.

There is indeed evidence that PPC activity predicts the sensory consequences of upcoming movements (Mulliken et al., 2008; Pilacinski et al., 2018; Sirigu et al., 1996) as well as sensorimotor prediction errors during motor learning (Savoie et al., 2018). Moreover, PPC activity predicts future eye position (Dowiasch et al., 2016). Medendorp and Heed confirm the idea that the PPC is engaged in the state estimation specifying the existence of a rostral body-related pole that projects the environment onto the body and a caudal environment-related pole that projects the body into an environment landscape (Figure 25B).

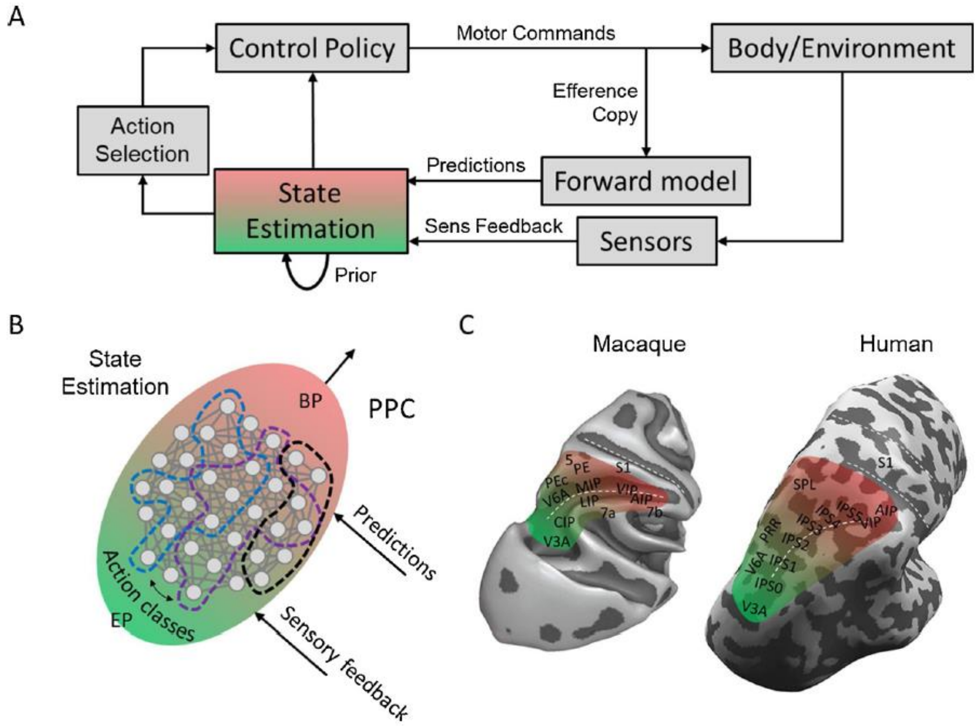

Figure 25. Illustration of optimal feedback control theory and its possible large-scale implementation in the brain. A. *Optimal Feedback Control (figure based on Shadmehr and Krakauer, 2008). The state estimator combines current sensory information with the predicted outcomes based on motor outputs (through a internal forward model) as well as information about the expected sensory state (the prior), accumulated over comparable circumstances. A process of action selection specifies the goal of the behavior, based on action clustered inputs of the state estimator. The control policy reflects a set of rules, including feedback gains, specifying how to act given the estimated current state of the body and world to perform the action.* ***B.*** *State estimation in PPC extends into a body-related (BP) and an environment-related pole (EP) along the rostral- caudal dimension. The medial-to-lateral gradient is dominated by action classes, involving interconnected neuronal networks, often involving the same units (see blue, purple and black dashed-tracings).* ***C.*** *Comparison of monkey and human PPC. Dashed lines indicate the central sulcus and the intraparietal sulcus (IPS), which divides the superior parietal (SPL) and inferior parietal lobule (IPL). Regions are shown on semi-inflated cortical surfaces, to also indicate regions in the bank of the IPS. In both species, the red-to-green gradient illustrates the rostral-to-caudal gradient for state estimation from a body-related to an environment-related pole (Reproduced from Medendorp and Heed, 2019).*

Therefore, the recent view is that perceptual and action-related functions are two sides of the same coin. The role of PPC is to estimate the state of body and environment, contributing to choose the next best action and supporting optimal control of its execution.

8. CONCLUSIONS

Present data show that eye- and arm-position modulation of neuronal activity is similar in areas V6A and PEc, and different in area PE. These results well agree with the recent suggestion that both V6A and PEc belong to Brodmann's area 7 while PE to Brodmann's area 5 (Gamberini et al., 2020).

According to this view, we found that all three SPL areas integrate eye and limb position signals during the hand holding at the end of a foveal reaching, but the influence of the two signals is different in areas V6A and PEc with respect to PE. Area PE was found to be more sensitive to limb proprioceptive input while PEc and V6A, particularly this latter, were also influenced by the direction of gaze.

The joint processing of eye and limb position signals that occurs in V6A and PEc and their known greater sensitivity to visual stimuli in comparison to PE could suggest a major role of these areas in the control of the hand position during voluntary movement. Noteworthy, a close association between the direction of the gaze, the visual location of the target and the perception of limb in the space is necessary to ensure a correct eye-hand coordination. Therefore, V6A and PEc are likely to combine eye and limb position information to guarantee a successful interaction with the desired object. The two signals are less correlated in PE which relies more on proprioception input, elaborating information of the limb status. This could find a parallel with the theory proposed by Medendorp and Heed (2019) in the PPC that see caudal areas as more involved in the processing of stimuli in relation to the environment (where purposeful actions take place) whereas rostral areas as PE in relation to the body in the space.

These data support the existence, often reported in literature (Piserchia et al., 2017; Gamberini et al., 2018; De Vitis et al., 2019; Impieri et al., 2019), of a functional trend in the SPL, with the anterior part more involved in limb representation and the posterior one showing visuomotor characteristics well suited to control goal-directed actions.

Another interpretation of the different encoding of eye and limb information in the SPL could be the influence of spatial attention directed to the target which may be stronger in caudal areas, in particular in V6A with respect to rostral ones.

According to the subdivision proposed that see V6A and PEc more similar with respect to PE, monkey and human SPL would be organized in a similar way (Figure 26).

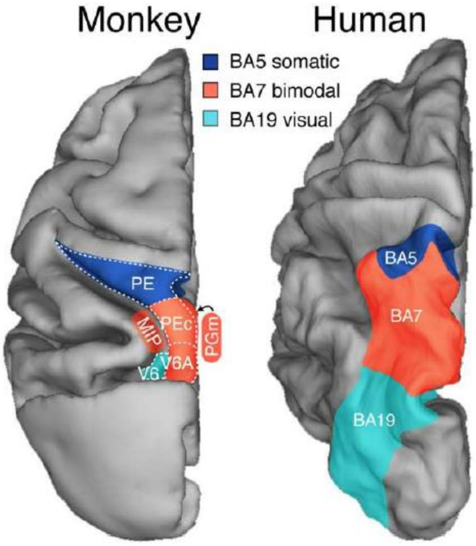

***Figure 26. Comparison between monkey and human SPLs**. Left, dorsal view of the left hemisphere of macaque brain showing the location and extent of a number of SPL areas: the region colored in light blue is the visual cortex (that includes area V6) and belongs to BA (Brodamann's Area) 19; the region colored in orange, which includes areas PEc, V6A, MIP, and PGm, is responsive to both visual and somatosensory stimulations and belongs to BA7; the region colored in blue (that includes area PE) is responsive to somatosensory stimulations but not visual stimulations, and belongs to BA5. Right, dorsal view of the left hemisphere of the human brain showing the location and extent of BA5 (blue), 7 (orange), and 19 (light blue) (from Gamberini et al. 2021).*

The shared functional and anatomical features in human and non-human primates address future investigations on the possible implementation of brain-machine interfaces with neural signals coming from the SPL with the aim of regaining motor function in tetraplegic subjects.

9. REFERENCES

Abrams, R. A., Meyer, D. E., & Kornblum, S. (1990). Eye-hand coordination: oculomotor control in rapid aimed limb movements. Journal of Experimental Psychology. Human Perception and Performance, 16(2), 248–267. https://doi.org/10.1037//0096-1523.16.2.248

Albert, S. T., Hadjiosif, A. M., Jang, J., Zimnik, A. J., Soteropoulos, D. S., Baker, S. N., Churchland, M. M., Krakauer, J. W., & Shadmehr, R. (2020). Postural control of arm and fingers through integration of movement commands. ELife, 9. https://doi.org/10.7554/ELIFE.52507

Andersen, R. A., Asanuma, C., Essick, G., & Siegel, R. M. (1990). Corticocortical connections of anatomically and physiologically defined subdivisions within the inferior parietal lobule. The Journal of comparative neurology, 296(1), 65–113. https://doi.org/10.1002/cne.902960106

Andersen, R. A., & Buneo, C. A. (2002). Intentional maps in posterior parietal cortex. Annual review of neuroscience, 25, 189–220. https://doi.org/10.1146/annurev.neuro.25.112701.142922

Arsenault, J. T., Caspari, N., Vandenberghe, R., & Vanduffel, W. (2018). Attention shifts recruit the monkey default mode network. Journal of Neuroscience, 38(5), 1202–1217. https://doi.org/10.1523/JNEUROSCI.1111-17.2017

Bakola, S., Gamberini, M., Passarelli, L., Fattori, P., & Galletti, C. (2010). Cortical Connections of Parietal Field PEc in the Macaque: Linking Vision and Somatic Sensation for the Control of Limb Action. Cerebral Cortex, 20(11), 2592. https://doi.org/10.1093/cercor/bhq007

Bakola, S., Passarelli, L., Gamberini, M., Fattori, P., & Galletti, C. (2013). Cortical connectivity suggests a role in limb coordination for macaque area PE of the superior parietal cortex. Journal of Neuroscience, 33(15), 6648–6658. https://doi.org/10.1523/JNEUROSCI.4685-12.2013

Bartolo, A., Rossetti, Y., Revol, P., Urquizar, C., Pisella, L., & Coello, Y. (2018). Reachability judgement in optic ataxia: Effect of peripheral vision on hand and target perception in depth. Cortex, 98, 102–113. https://doi.org/10.1016/j.cortex.2017.05.013

Batista, A. P., Buneo, C. A., Snyder, L. H., & Andersen, R. A. (1999). Reach plans in eye-centered coordinates. Science (New York, N.Y.), 285(5425), 257–260. http://www.ncbi.nlm.nih.gov/pubmed/10398603

Battaglia-Mayer, A., Caminiti, R., Lacquaniti, F., & Zago, M. (2003). Multiple levels of representation of reaching in the parieto-frontal network. Cerebral Cortex (New York, N.Y. : 1991), 13(10), 1009–1022. https://doi.org/10.1093/CERCOR/13.10.1009

Battaglia-Mayer, A., Ferraina, S., Genovesio, A., Marconi, B., Squatrito, S., Molinari, M., Lacquaniti, F., & Caminiti, R. (2001). Eye-hand coordination during reaching. II. An analysis of the relationships between visuomanual signals in parietal cortex and parieto-frontal association projections. Cerebral Cortex (New York, N.Y. : 1991), 11(6), 528–544.

Battaglini, P. P., Muzur, A., Galletti, C., Skrap, M., Brovelli, A., & Fattori, P. (2002). Effects of lesions to area V6A in monkeys. Experimental brain research, 144(3), 419–422. https://doi.org/10.1007/s00221-002-1099-4

Bhattacharyya, R., Musallam, S., & Andersen, R. A. (2009). Parietal Reach Region Encodes Reach Depth Using Retinal Disparity and Vergence Angle Signals. Journal of Neurophysiology, 102(2), 805–816. https://doi.org/10.1152/jn.90359.2008

Borra, E., Gerbella, M., Rozzi, S., & Luppino, G. (2017). The macaque lateral grasping network: A neural substrate for generating purposeful hand actions. Neuroscience and Biobehavioral Reviews, 75, 65–90. https://doi.org/10.1016/J.NEUBIOREV.2017.01.017

Borra, E., Gerbella, M., Rozzi, S., Tonelli, S., & Luppino, G. (2014). Projections to the superior colliculus from inferior parietal, ventral premotor, and ventrolateral prefrontal areas involved in controlling goal-directed hand actions in the macaque. Cerebral Cortex (New York, N.Y. : 1991), 24(4), 1054–1065. https://doi.org/10.1093/CERCOR/BHS392

Breveglieri, R., Bosco, A., Galletti, C., Passarelli, L., & Fattori, P. (2016). Neural activity in the medial parietal area V6A while grasping with or without visual feedback. Scientific Reports, 6. https://doi.org/10.1038/SREP28893

Breveglieri, R., Galletti, C., Dal Bò, G., Hadjidimitrakis, K., Fattori, P., Dal Bò, G., Hadjidimitrakis, K., & Fattori, P. (2014). Multiple aspects of neural activity during reaching preparation in the medial posterior parietal area V6A. Journal of Cognitive Neuroscience, 26(4), 878–895. https://doi.org/10.1162/jocn_a_00510

Breveglieri, R., Galletti, C., Gamberini, M., Passarelli, L., & Fattori, P. (2006). Somatosensory cells in area PEc of macaque posterior parietal cortex. Journal of Neuroscience, 26(14), 3679–3684. https://doi.org/10.1523/JNEUROSCI.4637-05.2006

Breveglieri, R., Galletti, C., Monaco, S., & Fattori, P. (2008). Visual, somatosensory, and bimodal activities in the macaque parietal area PEc. Cerebral Cortex, 18(4), 806–816. https://doi.org/10.1093/CERCOR/BHM127

Breveglieri, R., Hadjidimitrakis, K., Bosco, A., Sabatini, SP., Galletti, C., & Fattori, P. (2012). Eye Position Encoding in Three-Dimensional Space: Integration of Version and Vergence Signals in the Medial Posterior Parietal Cortex. Journal of Neuroscience, 32(1), 159–169. https://doi.org/10.1523/JNEUROSCI.4028-11.2012

Bremmer,F., Distler,C. & Hoffmann,K.P.(1997). Eye position effects in monkey cortex. II. pursuit-and fixation-related activity in posterior parietal areas LIP and7A. J. Neurophysiol. 77, 962–977.

Buneo, C. A., Jarvis, M. R., Batista, A. P., & Andersen, R. A. (2002). Direct visuomotor transformations for reaching. Nature, 416(6881), 632–636. https://doi.org/10.1038/416632a

Caminiti, R., Innocenti, G. M., & Battaglia-Mayer, A. (2015). Organization and evolution of parieto-frontal processing streams in macaque monkeys and humans. Neuroscience & Biobehavioral Reviews, 56, 73–96. https://doi.org/https://doi.org/10.1016/j.neubiorev.2015.06.014

Caminiti, R., Ferraina, S., & Mayer, A. B. (1998). Visuomotor transformations: early cortical mechanisms of reaching. Current opinion in neurobiology, 8(6), 753–761. https://doi.org/10.1016/s0959-4388(98)80118-9

Caspari, N., Arsenault, J. T., Vandenberghe, R., & Vanduffel, W. (2018). Functional Similarity of Medial Superior Parietal Areas for Shift-Selective Attention Signals in Humans and Monkeys. Cerebral Cortex, 28(6), 2085–2099. https://doi.org/10.1093/cercor/bhx114

Caspari, N., Janssens, T., Mantini, D., Vandenberghe, R., & Vanduffel, W. (2015). Covert Shifts of Spatial Attention in the Macaque Monkey. Journal of Neuroscience, 35(20), 7695–7714. https://doi.org/10.1523/JNEUROSCI.4383-14.2015

Cheney, P. D., & Fetz, E. E. (1980). Functional classes of primate corticomotoneuronal cells and their relation to active force. Journal of Neurophysiology, 44(4), 773–791. https://doi.org/10.1152/jn.1980.44.4.773

Ciavarro, M., Ambrosini, E., Tosoni, A., Committeri, G., Fattori, P., & Galletti, C. (2013). rTMS of Medial Parieto-occipital Cortex Interferes with Attentional Reorienting during Attention and Reaching Tasks. Journal of Cognitive Neuroscience, 25(9), 1453–1462. https://doi.org/10.1162/jocn_a_00409

Cohen, D. A. D., Prud'homme, M. J. L., & Kalaska, J. F. (1994). Tactile activity in primate primary somatosensory cortex during active arm movements: correlation with receptive field properties. Journal of Neurophysiology, 71(1), 161–172. https://doi.org/10.1152/JN.1994.71.1.161

Colby, C. L., & Goldberg, M. E. (1999). Space and attention in parietal cortex. Annual review of neuroscience, 22, 319–349. https://doi.org/10.1146/annurev.neuro.22.1.319

Crammond, D. J., & Kalaska, J. F. (1989). Neuronal activity in primate parietal cortex area 5 varies with intended movement direction during an instructed-delay period. Experimental Brain Research, 76(2), 458–462. https://doi.org/10.1007/BF00247902

Cui, H., & Andersen, R. A. (2011). Different Representations of Potential and Selected Motor Plans by Distinct Parietal Areas. Journal of Neuroscience, 31(49), 18130–18136. https://doi.org/10.1523/JNEUROSCI.6247-10.2011

De Vitis, M., Breveglieri, R., Hadjidimitrakis, K., Vanduffel, W., Galletti, C., & Fattori, P. (2019). The neglected medial part of macaque area PE: segregated processing of reach depth and direction. Brain Structure and Function, 224(7), 2537–2557. https://doi.org/10.1007/S00429-019-01923-8

Diomedi, S., Vaccari, F. E., Filippini, M., Fattori, P., & Galletti, C. (2020). Mixed Selectivity in Macaque Medial Parietal Cortex during Eye-Hand Reaching. IScience, 23(10), 101616. https://doi.org/10.1016/j.isci.2020.101616

Donaldson, I. M. L. (2000). The functions of the proprioceptors of eye muscles. Philos. Trans. R. Soc. Lond. B Biol. Sci. 355, 1685–1754.

Dowiasch, S., Blohm, G., & Bremmer, F. (2016). Neural correlate of spatial (mis-)localization during smooth eye movements. European Journal of Neuroscience, 44(2), 1846–1855. https://doi.org/10.1111/EJN.13276

Duffy, F. H., & Burchfiel, J. L. (1971). Somatosensory system: organizational hierarchy from single units in monkey area 5. Science, 172(3980), 273–275. https://doi.org/10.1126/science.172.3980.273

Evarts, E. v. (1969). Activity of pyramidal tract neurons during postural fixation. Journal of Neurophysiology, 32(3), 375–385. https://doi.org/10.1152/jn.1969.32.3.375

Fattori, P., Breveglieri, R., Bosco, A., Gamberini, M., & Galletti, C. (2017). Vision for Prehension in the Medial Parietal Cortex. Cerebral cortex (New York, N.Y. : 1991), 27(2), 1149–1163. https://doi.org/10.1093/cercor/bhv302

Fattori, P., Breveglieri, R., Marzocchi, N., Filippini, D., Bosco, A., & Galletti, C. (2009a). Hand Orientation during Reach-to-Grasp Movements Modulates Neuronal Activity in the Medial Posterior Parietal Area V6A. The Journal of Neuroscience, 29(6), 1928–1936. https://doi.org/10.1523/JNEUROSCI.4998-08.2009

Fattori, P., Breveglieri, R., Marzocchi, N., Filippini, D., Bosco, A., & Galletti, C. (2009b). Hand orientation during reach-to-grasp movements modulates neuronal activity in the medial posterior parietal area V6A. Journal of Neuroscience, 29(6), 1928–1936. https://doi.org/10.1523/JNEUROSCI.4998-08.2009

Fattori, P., Gamberini, M., Kutz, D. F., & Galletti, C. (2001). 'Arm-reaching' neurons in the parietal area V6A of the macaque monkey. European Journal of Neuroscience, 13(12), 2309–2313. https://doi.org/10.1046/j.0953-816x.2001.01618.x

Fattori, P., Kutz, D. F., Breveglieri, R., Marzocchi, N., & Galletti, C. (2005). Spatial tuning of reaching activity in the medial parieto-occipital cortex (area V6A) of macaque monkey. European Journal of Neuroscience, 22(4), 956–972. https://doi.org/10.1111/J.1460-9568.2005.04288.X

Fattori, P., Raos, V., Breveglieri, R., Bosco, A., Marzocchi, N., & Galletti, C. (2010). The dorsomedial pathway is not just for reaching: Grasping neurons in the medial parieto-occipital cortex of the macaque monkey. Journal of Neuroscience, 30(1), 342–349. https://doi.org/10.1523/JNEUROSCI.3800-09.2010

Ferraina, S., Battaglia-Mayer, A., Genovesio, A., Marconi, B., Onorati, P., & Caminiti, R. (2001). Early coding of visuomanual coordination during reaching in parietal area PEc. Journal of Neurophysiology, 85(1), 462–467.

Ferraina, S., Battaglia-Mayer, A., Genovesio, A., Archambault, P., & Caminiti, R. (2009). Parietal encoding of action in depth. Neuropsychologia, 47, 1409–1420. https://doi.org/10.1016/j.neuropsychologia.2008.12.028

Fluet, M. C., Baumann, M. A., & Scherberger, H. (2010). Context-specific grasp movement representation in macaque ventral premotor cortex. Journal of Neuroscience, 30(45), 15175–15184. https://doi.org/10.1523/JNEUROSCI.3343-10.2010

Rizzolatti, G., Fadiga, L., Fogassi, L., & Gallese, V. (1997). The space around us. Science (New York, N.Y.), 277(5323), 190–191. https://doi.org/10.1126/science.277.5323.190

Fromm, C. (1983). Changes of steady state activity in motor cortex consistent with the length-tension relation of muscle. Pflügers Archiv European Journal of Physiology, 398(4), 318–323. https://doi.org/10.1007/BF00657241

Galletti, C., Battaglini, P. P., & Fattori, P. (1995). Eye position influence on the parieto-occipital area PO (V6) of the macaque monkey. European Journal of Neuroscience, 7(12), 2486–2501. https://doi.org/10.1111/j.1460-9568.1995.tb01047.x

Galletti, C., Breveglieri, R., Lappe, M., Bosco, A., Ciavarro, M., & Fattori, P. (2010). Covert shift of attention modulates the ongoing neural activity in a reaching area of the macaque dorsomedial visual stream. PLoS ONE, 5(11). https://doi.org/10.1371/JOURNAL.PONE.0015078

Galletti, C., & Fattori, P. (2018). The dorsal visual stream revisited: Stable circuits or dynamic pathways? Cortex, 98, 203–217. https://doi.org/10.1016/j.cortex.2017.01.009

Galletti, C., Fattori, P., Gamberini, M., & Kutz, D. F. (1999b). The cortical visual area V6: brain location and visual topography. *The European journal of neuroscience*, *11*(11), 3922–3936. https://doi.org/10.1046/j.1460-9568.1999.00817.x

Galletti, C., Fattori, P., Kutz, D. F., & Gamberini, M. (1999a). Brain location and visual topography of cortical area V6A in the macaque monkey. *The European journal of neuroscience*, *11*(2), 575–582. https://doi.org/10.1046/j.1460-9568.1999.00467.x

Galletti, C., Gamberini, M., & Fattori, P. (2022). The posterior parietal area V6A: An attentionally-modulated visuomotor region involved in the control of reach-to-grasp action. *Neuroscience and biobehavioral reviews*, *141*, 104823.

Galletti, C., Kutz, D. F., Gamberini, M., Breveglieri, R., & Fattori, P. (2003). Role of the medial parieto-occipital cortex in the control of reaching and grasping movements. Experimental Brain Research, 153(2), 158–170. https://doi.org/10.1007/S00221-003-1589-Z

Gamberini, M., Dal Bò, G., Breveglieri, R., Briganti, S., Passarelli, L., Fattori, P., & Galletti, C. (2018). Sensory properties of the caudal aspect of the macaque's superior parietal lobule. Brain Structure and Function, 223(4), 1863–1879. https://doi.org/10.1007/S00429-017-1593-X

Gamberini, M., Galletti, C., Bosco, A., Breveglieri, R., & Fattori, P. (2011). Is the medial posterior parietal area V6A a single functional area? Journal of Neuroscience, 31(13), 5145–5157. https://doi.org/10.1523/JNEUROSCI.5489-10.2011

Gamberini, M., Passarelli, L., Fattori, P., & Galletti, C. (2020). Structural connectivity and functional properties of the macaque superior parietal lobule. Brain Structure and Function, 225(4), 1349–1367. https://doi.org/10.1007/s00429-019-01976-9

Gamberini, M., Passarelli, L., Fattori, P., Zucchelli, M., Bakola, S., Luppino, G., & Galletti, C. (2009). Cortical connections of the visuomotor parietooccipital area V6Ad of the macaque monkey. Journal of Comparative Neurology, 513(6), 622–642. https://doi.org/10.1002/cne.21980

Gamberini, M., Passarelli, L., Filippini, M., Fattori, P., & Galletti, C. (2021). Vision for action: thalamic and cortical inputs to the macaque superior parietal lobule. Brain Structure and Function, 226(9), 2951–2966. https://doi.org/10.1007/s00429-021-02377-7

Gardner, E. P., & Costanzo, R. M. (1981). Properties of kinesthetic neurons in somatosensory cortex of awake monkeys. Brain research, 214(2), 301–319. https://doi.org/10.1016/0006-8993(81)91196-3

Gardner, E. P., Ro, J. Y., Babu, K. S., & Ghosh, S. (2007). Neurophysiology of prehension. II. Response diversity in primary somatosensory (SI) and motor (MI) cortices. Journal of Neurophysiology, 97(2), 1656–1670. https://doi.org/10.1152/jn.01031.2006

Georgopoulos, A. P., Caminiti, R., & Kalaska, J. F. (1984). Static spatial effects in motor cortex and area 5: Quantitative relations in a two-dimensional space. Experimental Brain Research, 54(3), 446–454. https://doi.org/10.1007/BF00235470

Genovesio, A., & Ferraina, S. (2004). Integration of retinal disparity and fixation-distance related signals toward an egocentric coding of distance in the posterior parietal cortex of primates. Journal of neurophysiology, 91(6), 2670–2684. https://doi.org/10.1152/jn.00712.2003

Ghez, C., Scheidt, R., & Heijink, H. (2007). Different learned coordinate frames for planning trajectories and final positions in reaching. Journal of Neurophysiology, 98(6), 3614–3626. https://doi.org/10.1152/JN.00652.2007/ASSET/IMAGES/LARGE/Z9K0110785140006.JPEG

Goodale, M. A., & Milner, A. D. (1992). Separate visual pathways for perception and action. Trends in neurosciences, 15(1), 20–25. https://doi.org/10.1016/0166-2236(92)90344-8

Guo, J. Z., Graves, A. R., Guo, W. W., Zheng, J., Lee, A., Rodríguez-Gonzá Lez, J., Li, N., Macklin, J. J., Phillips, J. W., Mensh, B. D., Branson, K., & Hantman, A. W. (2015). Cortex commands the performance of skilled movement. ELife, 4(DECEMBER2015). https://doi.org/10.7554/ELIFE.10774

Hadjidimitrakis K, Bertozzi F, Breveglieri R, Bosco A, Galletti C, Fattori P (2014a) Common neural substrate for processing depth and direction signals for reaching in the monkey medial posterior parietal cortex. Cereb Cortex 24:1645–1657. https://doi.org/10.1093/cercor/bht021

Hadjidimitrakis K, Bertozzi F, Breveglieri R, Fattori P, Galletti C (2014b) Body-centered, mixed, but not hand-centered coding of visual targets in the medial posterior parietal cortex during reaches in 3D space. Cereb Cortex 24:3209–3220. https://doi.org/10.1093/cercor/bht181

Hadjidimitrakis, K., Breveglieri, R., Placenti, G., Bosco, A., Sabatini, S. P., & Fattori, P. (2011). Fix Your Eyes in the Space You Could Reach: Neurons in the Macaque Medial Parietal Cortex Prefer Gaze Positions in Peripersonal Space. PLoS ONE, 6(8), e23335. https://doi.org/10.1371/journal.pone.0023335

Hadjidimitrakis, K., Dal Bo', G., Breveglieri, R., Galletti, C., & Fattori, P. (2015). Overlapping representations for reach depth and direction in caudal superior parietal lobule of macaques. Journal of Neurophysiology, 114(4), 2340–2352. https://doi.org/10.1152/jn.00486.2015

Hamel-Pâquet, C., Sergio, L. E., & Kalaska, J. F. (2006). Parietal area 5 activity does not reflect the differential time-course of motor output kinetics during arm-reaching and isometric-force tasks. Journal of Neurophysiology, 95(6), 3353–3370. https://doi.org/10.1152/jn.00789.2005

Helmholtz von H. (1866). Handbuch der Physiologischen Optik (Part III). Leipzig: Voss.

Hyvärinen, J., & Poranen, A. (1978). Receptive field integration and submodality convergence in the hand area of the post-central gyrus of the alert monkey. The Journal of physiology, 283, 539–556. https://doi.org/10.1113/jphysiol.1978.sp012518

Huang, R. S., & Sereno, M. I. (2018). Multisensory and sensorimotor maps. Handbook of Clinical Neurology, 151, 141–161. https://doi.org/10.1016/B978-0-444-63622-5.00007-3

Iwamura, Y., Tanaka, M., Sakamoto, M. & O. Hikosaka (1983). Converging patterns of finger representation and complex response properties of neurons in area 1 of the first somatosensory cortex of the conscious monkey. Exp Brain Res 51, 327–337. https://doi.org/10.1007/BF00237869

Iwamura, Y., & Tanaka, M. (1978). Postcentral neurons in hand region of area 2: Their possible role in the form discrimination of tactile objects. Brain Research, 150(3), 662–666. https://doi.org/10.1016/0006-8993(78)90834-X

Impieri, D., Zilles, K., Niu, M., Rapan, L., Schubert, N., Galletti, C., & Palomero-Gallagher, N. (2019). Receptor density pattern confirms and enhances the anatomic-functional features of the macaque superior parietal lobule areas. Brain Structure and Function, 224(8), 2733–2756. https://doi.org/10.1007/S00429-019-01930-9

Johnson, P. B., Ferraina, S., Bianchi, L., & Caminiti, R. (1996). Cortical networks for visual reaching: physiological and anatomical organization of frontal and parietal lobe arm regions. Cerebral Cortex, 6(2), 102–119. http://www.ncbi.nlm.nih.gov/pubmed/8670643

Jeannerod, M., Arbib, M. A., Rizzolatti, G., & Sakata, H. (1995). Grasping objects: the cortical mechanisms of visuomotor transformation. Trends in neurosciences, 18(7), 314–320.

Jones, E. G., Coulter, J. D., & Hendry, S. H. (1978). Intracortical connectivity of architectonic fields in the somatic sensory, motor and parietal cortex of monkeys. The Journal of Comparative Neurology, 181(2), 291–347. https://doi.org/10.1002/cne.901810206

Jones, E. G., & Powell, T. P. (1970). An anatomical study of converging sensory pathways within the cerebral cortex of the monkey. Brain : A Journal of Neurology, 93(4), 793–820. http://www.ncbi.nlm.nih.gov/pubmed/4992433

Kalaska, J. F. (1994). Central neural mechanisms of touch and proprioception. Canadian Journal of Physiology and Pharmacology, 72(5), 542–545. https://doi.org/10.1139/Y94-078

Kalaska, J. F., & Hyde, M. L. (1985). Area 4 and area 5: differences between the load direction-dependent discharge variability of cells during active postural fixation. Experimental Brain Research, 59(1), 197–202. http://www.ncbi.nlm.nih.gov/pubmed/3926528

Kalaska, J. F., Scott, S. H., Cisek, P., & Sergio, L. E. (1997). Cortical control of reaching movements. Current Opinion in Neurobiology, 7(6), 849–859. https://doi.org/10.1016/S0959-4388(97)80146-8

Kandel E, Schwartz J, Jessel T, Siegelbaum S, Hudspeth AJ (2014) Principles of Neural Science, Fifth Edition.

Karnath, H. O., & Perenin, M. T. (2005). Cortical control of visually guided reaching: evidence from patients with optic ataxia. *Cerebral cortex (New York, N.Y. : 1991)*, *15*(10), 1561–1569. https://doi.org/10.1093/cercor/bhi034

Kelley, T. A., Serences, J. T., Giesbrecht, B., & Yantis, S. (2008). Cortical mechanisms for shifting and holding visuospatial attention. Cerebral Cortex (New York, N.Y. : 1991), 18(1), 114–125. https://doi.org/10.1093/cercor/bhm036

Khan, A. Z., Crawford, J. D., Blohm, G., Urquizar, C., Rossetti, Y., & Pisella, L. (2007). Influence of initial hand and target position on reach errors in optic ataxic and normal subjects. Journal of Vision, 7(5), 8–8. https://doi.org/10.1167/7.5.8

Kutz, D. F., Fattori, P., Gamberini, M., Breveglieri, R., & Galletti, C. (2003). Early- and late-responding cells to saccadic eye movements in the cortical area V6A of macaque monkey. Experimental Brain Research Experimentelle Hirnforschung Expérimentation Cérébrale, 149(1), 83–95. https://doi.org/10.1007/s00221-002-1337-9

Kutz, D. F., Marzocchi, N., Fattori, P., Cavalcanti, S., & Galletti, C. (2005). Real-time supervisor system based on trinary logic to control experiments with behaving animals and humans. Journal of Neurophysiology, 93(6), 3674–3686. https://doi.org/10.1152/jn.01292.2004

Lacquaniti, F., Guigon, E., Bianchi, L., Ferraina, S., & Caminiti, R. (1995). Representing spatial information for limb movement: role of area 5 in the monkey. Cerebral Cortex, 5(5), 391–409. http://www.ncbi.nlm.nih.gov/pubmed/8547787

Lametti, D. R., Houle, G., & Ostry, D. J. (2007). Control of movement variability and the regulation of limb impedance. Journal of Neurophysiology, 98(6), 3516–3524. https://doi.org/10.1152/JN.00970.2007/ASSET/IMAGES/LARGE/Z9K0120785740006.JPEG

Land MF, Hayhoe M (2001) In what ways do eye movements contribute to everyday activities? Vision Res 41:3559–3565.

Marzocchi, N., Breveglieri, R., Galletti, C., & Fattori, P. (2008). Reaching activity in parietal area V6A of macaque: Eye influence on arm activity or retinocentric coding of reaching movements? European Journal of Neuroscience, 27(3), 775–789. https://doi.org/10.1111/J.1460-9568.2008.06021.X

Matelli, M., & Luppino, G. (2001). Parietofrontal circuits for action and space perception in the macaque monkey. NeuroImage, 14(1 Pt 2). https://doi.org/10.1006/NIMG.2001.0835

Matelli, M., Luppino, G., & Rizzolatti, G. (1985). Patterns of cytochrome oxidase activity in the frontal agranular cortex of the macaque monkey. Behavioural Brain Research, 18(2), 125–136. https://doi.org/10.1016/0166-4328(85)90068-3

McGuire, L. M. M., & Sabes, P. N. (2011). Heterogeneous representations in the superior parietal lobule are common across reaches to visual and proprioceptive targets. The Journal of Neuroscience : The Official Journal of the Society for Neuroscience, 31(18), 6661–6673. https://doi.org/10.1523/JNEUROSCI.2921-10.2011

Medendorp, W. P., Goltz, H. C., Crawford, J. D., & Vilis, T. (2005). Integration of target and effector information in human posterior parietal cortex for the planning of action. Journal of Neurophysiology, 93(2), 954–962. https://doi.org/10.1152/JN.00725.2004

Medendorp, W. P., Goltz, H. C., Vilis, T., & Crawford, J. D. (2003). Gaze-centered updating of visual space in human parietal cortex. The Journal of Neuroscience : The Official Journal of the Society for Neuroscience, 23(15), 6209–6214. https://doi.org/10.1523/JNEUROSCI.23-15-06209.2003

Medendorp, W. P., & Heed, T. (2019). State estimation in posterior parietal cortex: Distinct poles of environmental and bodily states. Progress in Neurobiology, 183. https://doi.org/10.1016/J.PNEUROBIO.2019.101691

Milner AD, Goodale MA. 1995. The visual brain in action. Oxford:Oxford Press.

Molenberghs, P., Mesulam, M. M., Peeters, R., & Vandenberghe, R. R. C. (2007). Remapping Attentional Priorities: Differential Contribution of Superior Parietal Lobule and Intraparietal Sulcus. Cerebral Cortex, 17(11), 2703–2712. https://doi.org/10.1093/cercor/bhl179

Mountcastle, V. B., Lynch, J. C., Georgopoulos, A., Sakata, H., & Acuna, C. (1975). Posterior parietal association cortex of the monkey: command functions for operations within extrapersonal space. Journal of Neurophysiology, 38(4), 871–908. https://doi.org/10.1152/jn.1975.38.4.871

Mulliken, G. H., Musallam, S., & Andersen, R. A. (2008). Forward estimation of movement state in posterior parietal cortex. Proceedings of the National Academy of Sciences of the United States of America, 105(24), 8170–8177. https://doi.org/10.1073/PNAS.0802602105/SUPPL_FILE/0802602105SI.PDF

Nakamura, K., Chung, H. H., Graziano, M. S., & Gross, C. G. (1999). Dynamic representation of eye position in the parieto-occipital sulcus. Journal of neurophysiology, 81(5), 2374–2385. https://doi.org/10.1152/jn.1999.81.5.2374

Padberg, J., Franca, J. G., Cooke, D. F., Soares, J. G. M., Rosa, M. G. P., Fiorani, M., Gattass, R., & Krubitzer, L. (2007). Parallel evolution of cortical areas involved in skilled hand use. The Journal of Neuroscience : The Official Journal of the Society for Neuroscience, 27(38), 10106–10115. https://doi.org/10.1523/JNEUROSCI.2632-07.2007

Passarelli, L., Rosa, M. G. P., Gamberini, M., Bakola, S., Burman, K. J., Fattori, P., & Galletti, C. (2011). Cortical connections of area V6Av in the Macaque: A visual-input node to the eye/hand coordination system. Journal of Neuroscience, 31(5), 1790–1801. https://doi.org/10.1523/JNEUROSCI.4784-10.2011

Perenin, M. T., & Vighetto, A. (1988). Optic ataxia: a specific disruption in visuomotor mechanisms. I. Different aspects of the deficit in reaching for objects. Brain : a journal of neurology, 111 (Pt 3), 643–674. https://doi.org/10.1093/brain/111.3.643

Petrides, M., & Pandya, D. N. (1984). Projections to the frontal cortex from the posterior parietal region in the rhesus monkey. The Journal of Comparative Neurology, 228(1), 105–116. https://doi.org/10.1002/CNE.902280110

Pearson, R. C., & Powell, T. P. (1985). The projection of the primary somatic sensory cortex upon area 5 in the monkey. *Brain research*, *356*(1), 89–107. https://doi.org/10.1016/0165-0173(85)90020-7

Pilacinski, A., Wallscheid, M., & Lindner, A. (2018). Human posterior parietal and dorsal premotor cortex encode the visual properties of an upcoming action. PLOS ONE, 13(10), e0198051. https://doi.org/10.1371/JOURNAL.PONE.0198051

Piserchia, V., Breveglieri, R., Hadjidimitrakis, K., Bertozzi, F., Galletti, C., & Fattori, P. (2017). Mixed body/hand reference frame for reaching in 3D space in macaque parietal area PEc. Cerebral Cortex, 27(3), 1976–1990. https://doi.org/10.1093/CERCOR/BHW039

Pitzalis, S., Galletti, C., Huang, R. S., Patria, F., Committeri, G., Galati, G., Fattori, P., & Sereno, M. I. (2006). Wide-field retinotopy defines human cortical visual area V6. Journal of Neuroscience, 26(30), 7962–7973. https://doi.org/10.1523/JNEUROSCI.0178-06.2006

Pitzalis, S., Serra, C., Sulpizio, V., di Marco, S., Fattori, P., Galati, G., & Galletti, C. (2019). A putative human homologue of the macaque area PEc. NeuroImage, 202. https://doi.org/10.1016/j.neuroimage.2019.116092

Powell, T. & Mountcastle, V. B. (1959). Some aspects of the functional organization of the cortex of the postcentral *gyrus of the monkey: a correlation of findings obtained in a single unit analysis with cytoarchitecture. Bulletin of the Johns Hopkins Hospital, 105, 133–162.*

Prablanc, C., Echallier, J. F., Komilis, E., & Jeannerod, M. (1979). Optimal response of eye and hand motor systems in pointing at a visual target - I. Spatio-temporal characteristics of eye and hand movements and their relationships when varying the amount of visual information. Biological Cybernetics, 35(2), 113–124. https://doi.org/10.1007/BF00337436

Rizzolatti, G., & Matelli, M. (2003). Two different streams form the dorsal visual system: anatomy and functions. Experimental Brain Research, 153(2), 146–157. https://doi.org/10.1007/S00221-003-1588-0

Rossetti, Y., Pisella, L., & McIntosh, R. D. (2019). Definition: Optic ataxia. In Cortex (Vol. 121, p. 481). Masson SpA. https://doi.org/10.1016/j.cortex.2019.09.004

Ryan, C. P., Bettelani, G. C., Ciotti, S., Parise, C., Moscatelli, A., & Bianchi, M. (2021). The interaction between motion and texture in the sense of touch. Journal of neurophysiology, 126(4), 1375–1390. https://doi.org/10.1152/jn.00583.2020

Sakata, H., Takaoka, Y., Kawarasaki, A., & Shibutani, H. (1973). Somatosensory properties of neurons in the superior parietal cortex (area 5) of the rhesus monkey. Brain Research, 64(C), 85–102. https://doi.org/10.1016/0006-8993(73)90172-8

Sakata, H., Shibutani, H., & Kawano, K. (1980). Spatial properties of visual fixation neurons in posterior parietal association cortex of the monkey. Journal of neurophysiology, 43(6), 1654–1672. https://doi.org/10.1152/jn.1980.43.6.1654

Scheperjans, F., Grefkes, C., Palomero-Gallagher, N., Schleicher, A., & Zilles, K. (2005). Subdivisions of human parietal area 5 revealed by quantitative receptor autoradiography: a parietal region between motor, somatosensory, and cingulate cortical areas. NeuroImage, 25(3), 975–992. https://doi.org/10.1016/J.NEUROIMAGE.2004.12.017

Scheperjans, F., Palomero-Gallagher, N., Grefkes, C., Schleicher, A., & Zilles, K. (2005). Transmitter receptors reveal segregation of cortical areas in the human superior parietal cortex: relations to visual and somatosensory regions. NeuroImage, 28(2), 362–379. https://doi.org/10.1016/J.NEUROIMAGE.2005.06.028

Seal, J., & Commenges, D. (1985). A quantitative analysis of stimulus- and movement-related responses in the posterior parietal cortex of the monkey. Experimental Brain Research, 58(1), 144–153. https://doi.org/10.1007/BF00238962

Shadmehr, R., & Krakauer, J. W. (2008). A computational neuroanatomy for motor control. Experimental Brain Research, 185(3), 359–381. https://doi.org/10.1007/S00221-008-1280-5

Sherrington, C. S. (1906). The integrative action of the nervous system. Yale University Press. https://doi.org/10.1037/13798-000

Sherrington, C. S. (1918). Observations on the sensual role of the proprioceptive nerve-supply of the extrinsic ocular muscles. Brain: A Journal of Neurology, 41, 332–342. https://doi.org/10.1093/brain/41.3-4.332

Shi, Y., Apker, G., & Buneo, C. A. (2013). Multimodal representation of limb endpoint position in the posterior parietal cortex. Journal of Neurophysiology, 109(8), 2097–2107. https://doi.org/10.1152/jn.00223.2012

Sirigu, A., Duhamel, J. R., Cohen, L., Pillon, B., Dubois, B., & Agid, Y. (1996). The Mental Representation of Hand Movements After Parietal Cortex Damage. Science, 273(5281), 1564–1566. https://doi.org/10.1126/SCIENCE.273.5281.1564

Soechting, J. F., & Flanders, M. (1989). Sensorimotor representations for pointing to targets in three-dimensional space. Journal of neurophysiology, 62(2), 582–594. https://doi.org/10.1152/jn.1989.62.2.582

Strick, P. L., & Kim, C. C. (1978). Input to primate motor cortex from posterior parietal cortex (area 5). I. Demonstration by retrograde transport. Brain Research, 157(2), 325–330. http://www.ncbi.nlm.nih.gov/pubmed/102409

Taira, M., Mine, S., Georgopoulos, A. P., Murata, A., & Sakata, H. (1990). Parietal cortex neurons of the monkey related to the visual guidance of hand movement. Experimental Brain Research, 83(1), 29–36. https://doi.org/10.1007/BF00232190

Taoka, M., Toda, T., & Iwamura, Y. (1998). Representation of the midline trunk, bilateral arms, and shoulders in the monkey postcentral somatosensory cortex. Experimental Brain Research, 123(3), 315–322. http://www.ncbi.nlm.nih.gov/pubmed/9860270

Todorov, E. (2004). Optimality principles in sensorimotor control. Nature Neuroscience 2004 7:9, 7(9), 907–915. https://doi.org/10.1038/nn1309

Todorov, E., & Jordan, M. I. (2002). Optimal feedback control as a theory of motor coordination. Nature Neuroscience 2002 5:11, 5(11), 1226–1235. https://doi.org/10.1038/nn963

Ungerleider, L. G., & Mishkin, M. (1982). Two cortical visual systems. http://dx.doi.org/10.2139/ssrn.1353746.

Vandenberghe, R., Gitelman, D. R., Parrish, T. B., & Mesulam, M. M. (2001). Functional specificity of superior parietal mediation of spatial shifting. NeuroImage, 14(3), 661–673. https://doi.org/10.1006/nimg.2001.0860

Vogt, C., Vogt, O., 1919. Allgemeinere ergebnisse unserer hirnforschung. Journal of Neurology and Psychology 25, 279–461.

Von Holst, E. (1954). Relations between the central nervous system and the peripheral organs. British Journal of Animal Behaviour, 2, 89–94. https://doi.org/10.1016/S0950-5601(54)80044-X

Von Bonin, G., and Bailey, P. (1947).The Neocortex of Macaca mulatta. Illinois Monographs in the Medical Sciences, Vol V.Urbana, Illinois: The University of Illinois Press.

Von Economo, C. (1929). ‘‘The frontal lobe,’’ in The Cytoarchitectonics of the Human Cerebral Cortex, ed H. Milford (London: Oxford University Press), 27–67.

Wist, E. R. (1972). Eye movements and space perception. Bibl. Ophthalmol. 82: 348-357,.

Yadav, V., & Sainburg, R. L. (2011). Motor lateralization is characterized by a serial hybrid control scheme. Neuroscience, 196, 153–167. https://doi.org/10.1016/J.NEUROSCIENCE.2011.08.039

Yantis, S., Schwarzbach, J., Serences, J. T., Carlson, R. L., Steinmetz, M. A., Pekar, J. J., & Courtney, S. M. (2002). Transient neural activity in human parietal cortex during spatial attention shifts. Nature Neuroscience, 5(10), 995–1002. https://doi.org/10.1038/nn921

Zar, J. H. (1999). Biostatistical analysis. Prentice Hall.

Zarzecki, P., Shinoda, Y., & Asanuma, H. (1978). Projection from area 3a to the motor cortex by neurons activated from group I muscle afferents. Experimental Brain Research, 33(2), 269–282. https://doi.org/10.1007/BF00238065